Power Flow Studies of an AC-DC Transmission System

Ummaiah Bondhala

A Thesis Submitted to
Indian Institute of Technology Hyderabad
In Partial Fulfillment of the Requirements for
The Degree of Master of Technology

भारतीय प्रौद्योगिकी संस्थान हैदराबाद
Indian Institute of Technology Hyderabad

Department of Electrical Engineering

June 2011

Declaration

I declare that this written submission represents my ideas in my own words, and where ideas or words of others have been included, I have adequately cited and referenced the original sources. I also declare that I have adhered to all principles of academic honesty and integrity and have not misrepresented or fabricated or falsified any idea/data/fact/source in my submission. I understand that any violation of the above will be cause for disciplinary action by the Institute and can also evoke penal action from the sources that have thus not been properly cited, or from whom proper permission has not been taken when needed.

(Signature)

Ummaiah Bondhala

Student Name

EE09G012

Roll No

Approval Sheet

This thesis titled "Power Flow Studies of an AC-DC Transmission System" by Mr. Ummaiah Bondhala is approved for the degree of Master of Technology.

(Dr. P. V. Balasubramanyam) External Examiner
CPRI

(Dr. K. Siva Kumar) Internal Examiner
Dept. of Elec Eng
IITH

(Dr. Vaskar Sarkar) Research Supervisor
Dept. of Elec Eng
IITH

(Dr. R. Prasanth Kumar) Chairman
Dept. of Mech Eng
IITH

Acknowledgements

First I would like express my sincere gratitude to my supervisor Dr. Vaskar Sarkar for his help, sincere guidance, patience and constant encouragement, without which this thesis would not be possible to finish. The support i got from him through out my course work is invaluable.

I would like to express my gratitude to Dr. Ravinder David Koilpillai and faculty at IIT Hyderabad for their constant supervision as well as for providing necessary information regarding the project.

I would also like to thank the Indian Institute of Technology Hyderabad College for their generous support and providing peaceful environment to complete my work.

My thanks and appreciations also go to my friends and people who have willingly helped me out with their abilities.

At last but not the least, i wish to thank my parents and sisters for their unconditional love and support. They inspired me a lot and encouraged me to go my own way, without whom I would be unable to complete my course and thesis. special thanks to my brother Haranath.

Ummaiah Bondhala

To

My Parents and Sisters

Abstract

High Voltage Direct Current (HVDC) technology has characteristics that make it especially attractive for certain transmission applications. The same includes long-distance bulk power delivery, asynchronous interconnections, long submarine cable crossings and fast power controllability. Then, the HVDC transmission has proved its potential to be an interesting alternative or complement to the AC transmission.

The thesis presents Newton - Raphson method for the load flow analysis modified to achieve compatibility for AC - DC systems with the integrated DC link in the AC network. The elements of the Jacobian for the AC network are modified to include DC real and reactive power at the AC - DC buses, and their dependency on the a.c system variables. The DC equations such as voltage expressions at rectifier and inverter, network configuration equation *i.e., point-to-point, multiterminal series connection or multiterminal radial connection*, real and reactive power demands at converters are represented in a per unit form which will be compatible with per unit a.c equations. For various control strategies, simulations are carried out for point-to-point DC link and multiterminal DC links.

Simulations are also carried out for optimization of total power generation cost with the help of GAMS (General Algebraic Modeling System) and MATLAB for point-to-point and multiterminal HVDC transmission system. All equality and inequality constraints are considered in this optimization so that the entire power system can remain intact during the real-time operation.

Contents

List of Figures

List of Tables

Nomenclature

List of Symbols

α	Delay firing angle.
γ	Extinctison advance angle.
V_{di}	Inverter output voltage.
P_{di}	Power at inverter end.
I_d	Direct currrent.
$Y - Y$	Star-Star connection of transformer.
$Y - \Delta$	Star-Delta connection of transformer.
V_{dr}	Rectifier output voltage.
V_{do}	Rectifier output voltage at $\alpha = 0$.
L_c	Source inductance.
E_{LL}	RMS value of line to line voltage.
μ	Overlap angle.
δ	Extinction delay angle.
ϕ	Phase angle difference between voltage and current.
β	Ignition advance angle.

R_{dc}	DC line resistance.
P_{dr}	Power at rectifier end.
I_r	Direct current associated at rectifier end.
I_i	Direct current associated at inverter end.
t_{rec}	Transformer tap position associated at rectifier end.
t_{inv}	Transformer tap position associated at inverter end.
$p.u$	Per unit.
v	Voltage.
i	Current.
R	Resistance.
X	Reactance.
B	Suseptance.
P_{Gi}	Real power generation at i^{th} bus.
Q_{Gi}	Reactive power generation at i^{th} bus.
P_{Li}	Real power load at i^{th} bus.
Q_{Li}	Reactive power laod at i^{th} bus.
$Q_{min,i}$	Minimum reactive power limit at i^{th} bus.
$Q_{max,i}$	Maximum reactive power limit at i^{th} bus.
P_i	Net real power at i^th bus.
Q_i	Net reactive power at i^th bus.
P_{DC}	Active power associated with converter.

Q_{DC}	Reactive power associated with converter.
t_1	Transformer tap position associated with rectifier.
t_2	Transformer tap position associated with inverter.
$	Dollar.

List of Acronyms

HVDC	High Volatge Direct Current.
AC	Alternating Current.
DC	Direct Current.
GAMS	General Algebraic Modeling System.
MATLAB	MATrix LABoratory.
CSC	Current Source Converter.
VSC	Voltage Source Converter.
IGBT	Insulated Gate Bipolar Transistor .
PWM	Pulse Width Modulation.
HVDCPLUS	HVDC Power Link Universal System.
ELD	Economic Load Dispatch.
OPF	Optimal Power Flow.
SCR	Silicon Controlled Rectifier.
MW	Mega Watt.
MVAR	Mega Volt Ampere Reactive.

Chapter 1

Introduction

1.1 Background

Alternating current (AC) is widely used in industries and residential areas, but for the long transmission line (more than 600 Km) AC transmission is more expensive than direct current (DC). Technically, AC transmission line control is more complicated because of the frequency and dependency of power transfer on angle difference between the voltage phasors at the two ends. DC transmission does not have these limitations, which has led to build long High Voltage Direct Current (HVDC) transmission lines [1], [2]. HVDC technology is a high power electronics technology used in electric power systems to transfer bulk power over long distances. The DC transmission requires conversion at two ends, from AC to DC at the sending end and DC to AC at the receiving end. This conversion is done at converter stations. By simple control action, converter can be switched from rectifier to inverter and vice-versa. Thus facilitating power reversal.

The invention of the high voltage mercury valve shown the way towards the development of HVDC transmission. By 1954, the first commercial HVDC connecting two AC systems came in to operation in form of submarine cable link between the Swedish mainland and the island of Gotland [2]. Nowadays, the HVDC is being widely used all around the world. Until recently, HVDC based on thyristors uses the Current Source Converter (CSC) configuration. Now, a new type of HVDC transmission using more advanced semiconductor technology instead of thyristors is available for power conversion. The semiconductors used are Insulated Gate Bipolar Transistors (IGBTs) and the converters are voltage source converters (VSCs) which operate with high switching frequencies (1-2kHz) utilizing pulse width modulation (PWM). The technology is commercially available as HVDC Light or HVDCPLUS (Power Link Universal Systems) [3].

1.2 Literature survey

A brief introduction to the HVDC technology and the configurations like monopolar, bipolar, back to back and multiterminal with their operation are presented in [3], [4]. Figure 1.1 shows a simplified schematic picture of an HVDC system with the basic principle of transferring electric energy from one AC system or node to another in any direction. The

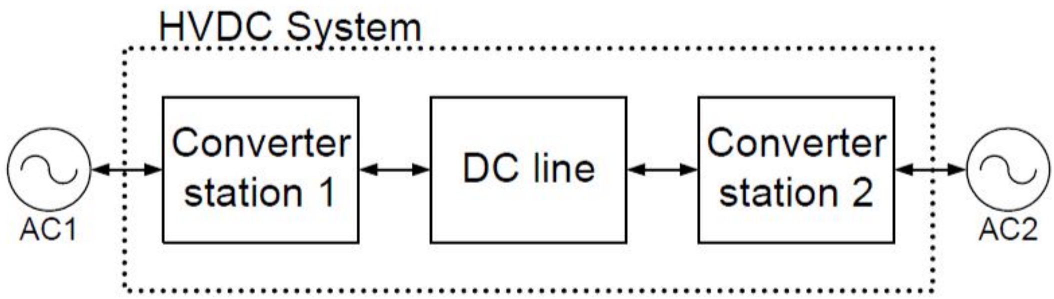

Figure 1.1: Schematic diagram of overall system with HVDC system

system consists of three blocks: two converter stations and a DC line. Each converter station has several components involved in power conversion. In [5], [6], analysis of Graetz bridge, which is used for AC/DC or DC/AC conversion, is explained with commutation and without commutation, and the equivalent circuit to represent HVDC line are presented. The following assumptions are made during the analysis.

(i) The valves of the converter are ideal and have no arc voltage drop.

(ii) AC source delivers a constant voltage and frequency.

(iii) The DC voltage and current have no ripple.

With the presence of DC link, the operating condition of the AC-DC system is defined as a.c bus voltage magnitudes, a.c bus voltage angles and DC variables. DC variables includes firing angles at converters, tap positions of the transformers located at converter stations, DC voltages at rectifier and inverter, and direct current through the line. Rectifier has minimum (α) limit of about 5^o to ensure adequate voltage across the valve before firing. Normally rectifier operates at a value between 15^o and 30^o so as to leave room for increasing voltage for power control. In case of inverter, it is necessary to maintain minimum extinction angle (γ) to avoid commutation failure [7]. Commutation failures are also caused because of the voltage dips due to a.c system faults, shift in phase angle of the line to line voltage and increase in the DC current because of faults at inverter side [8].

The primary functions of the DC control in a typical two terminal HVDC line are
(i) control of power flow between the terminals.
(ii) protect the equipment against the current/voltage.
HVDC control can be accomplished by gate control of valve firing angle or control of the ac voltage through tap changing of the converter transformer.

Modeling of AC-DC converter and the method used to include the equations for DC converters and transmission lines in a Newton Raphson AC system power flow are explained in [9]. The DC equations are presented in a per unit form that is compatible with the per unit AC equations. As a result of this conversion, the AC and DC equations can be solved simultaneously, rather than serially. This paper also includes the assumptions made in the derivation of the equations representing the AC-DC converter.

When the AC system includes an HVDC link, the equations of the power balance at the AC terminal are modified by including the powers at converter stations. The methods for load flow calculations of mixed AC-DC systems are grouped into three categories.

(i) H.A Sangavi and S.K Banarjee [10] proposed a sequential approach for carrying out the 1oad flow analysis of an integrated AC - DC power system. The particular method is based on solving the DC system and AC system equations separately.

(ii) In extended variables/unified method [11], [12], AC system and DC system are combined together and solved simultaneously. Because of its better computing efficiency and convergence it is more useful than sequential method in AC - DC power system.

(iii) Eliminated variable method [13], converters are treated as voltage dependent loads and the DC variables are eliminated from the power flow equations.

In [12], [14], more emphasis is placed on HVDC line control modes and suitable modification of conventional power flow jacobian matrix to include new elements contributed by the HVDC link. Control modes presented in [12] are, specifying firing angle α, the extinction angle γ, voltage at inverter side (V_{di}) and power at inverter side (P_{di}) is control mode A. Converter transformer taps are varied in order to meet these specifications. In Control mode B, the extinction angle γ is kept at its lower limit at the inverter, the transformer taps and the power P_{di} are specified. Power is controlled by varying the firing angle α at the rectifier. Firing angle (α) control is preferred to tap transformer, because of tap changer control is too slow. In control mode C, α is fixed to its minimum value and γ is regulated to maintain constant power. If the current I_d is kept constant instead of the power P_{di} , three other control modes are defined.

Concept of extending two terminal HVDC transmissions to multiterminal systems is briefly explained in [15], [16], [17]. It comprises classifications of multiterminal HVDC such as serial, radial and mesh connections, and their operation with their control characteristics. In a multiterminal transmission system, telecommunication is important for coordination of current level in different stations. A brief overview of DC line faults, AC faults and commutation failures are also discussed. A method for tapping energy from an intermediate point on an HVDC transmission line is presented in [18] has two main parts. The first one is the unit to extract power from the line that contains the conventional bridge and the second part of the station is the AC machine which provides the commutating voltage for the bridges.

In Economic Load Dispatch (ELD) [19] the demand is considered to be an aggregate parameter for the entire system. While load flow equations are introduced in ELD as a system of demand supply balance constraints, the optimum solution yields a set of decision variables satisfying desired objective (of cost minimization, loss minimization ....). Such a formulation is called as optimal power flow (OPF). OPF problem formulation with incorporation of HVDC link in a AC transmission system is explained in [20], [21]. This includes the vector of equality constraints such as power balance equations, inequality constraints such as upper and lower bounds of transmission line capacity, active and reactive power generation outputs and operating angles of converters.

1.3 Structure of thesis

Chapter 2 presents the different configurations of HVDC transmission system, main components of HVDC, rectifier and inverter analysis of Greatz circuit, advantages and disadvantages, applications of HVDC and principles of HVDC control .

Chapter 3 explains importance of power flow studies, formulation of load flow studies by Newton-Raphson method and inclusion of Direct current transmission line equations in power flow for both point-to-point and multiterminal transmission systems. Different control strategies for operation of AC DC transmission are also explained in this chapter. MATLAB simulations for both single and multiple HVDC transmission line are discussed.

Chapter 4 presents an Optimal Power Flow (OPF) model considering both AC and DC lines. Optimization of power generation cost is done with the help of General Algebraic Modeling System (GAMS) and MATLAB by including point-to-point and multiterminal HVDC lines in IEEE standard 14 bus system.

Chapter 5 Concludes the thesis and shows the road map for future work.

Chapter 2

HVDC Transmission System

2.1 Configurations of HVDC

HVDC converter bridges together with lines or cables can be arranged in a number of configurations [3], [4] as shown in Figs. 1.1 to 1.6

2.1.1 Monopolar HVDC system

In the monopolar configuration, two converters are connected by a single pole line and a positive or a negative DC voltage is used. In Fig. 2.1, there is only one insulated transmission conductor installed and the ground or sea provides the path for the return current. Alternatively, a metallic return conductor may be used as the return path where possible interference with underground/ underwater is objectionable.

2.1.2 Bipolar HVDC system

This is the most commonly used configuration of HVDC transmission systems. The bipolar configuration is shown in Fig. 2.2. It uses two insulated conductors as positive and negative poles. The two poles can be operated independently if both neutrals are grounded. The bipolar configuration increases the power transfer capacity. Under normal operation, the currents flowing in both poles are identical and there is no ground current. In case of failure of one pole, power transmission can continue in the other pole which

Figure 2.1: Monopolar HVDC link

increases the reliability.

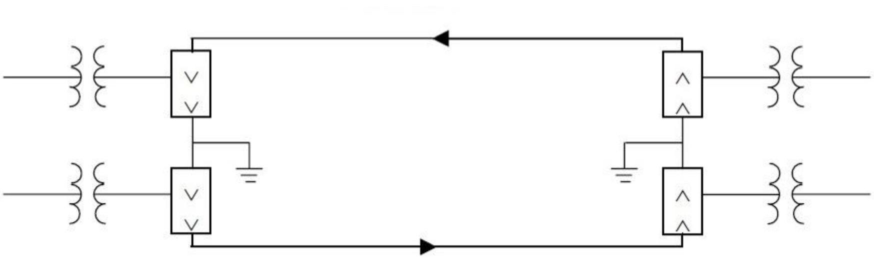

Figure 2.2: Bipolar HVDC link

2.1.3 Homopolar HVDC system

In the homopolar configuration, shown in Fig. 2.3. Here, two or more conductors have the negative polarity can be operated with ground or a metallic return. With two poles operated in parallel, the homopolar configuration reduces the insulation costs. However, the large earth return current is the major disadvantage.

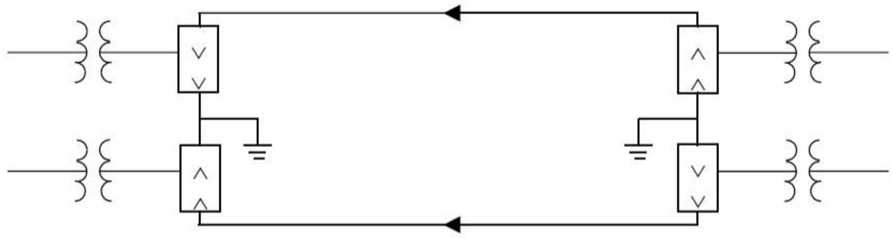

Figure 2.3: Homopolar HVDC link

2.1.4 Back-to-back HVDC system

This is the common configuration for connecting two adjacent asynchronous AC systems. Two converter stations are located at the same site and transmission line or cable is not needed. A block diagram of a back-to-back system is shown in Fig. 2.4. The two AC systems interconnected may have the same or different nominal frequencies.

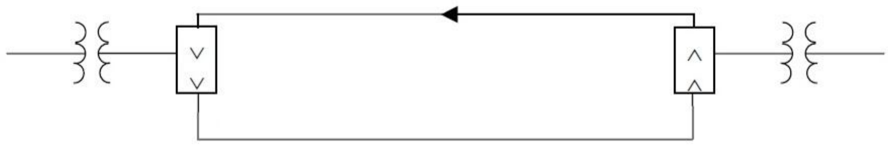

Figure 2.4: Back-to-back HVDC link

2.1.5 Multiterminal HVDC system

In the multiterminal configuration, three or more HVDC converter stations which are geographically separated are interconnected through transmission lines or cables. The system can be either parallel, where all converter stations are connected to the same voltage as shown in Fig. 2.5. or series multiterminal system, where one or more converter stations are connected in series as shown in Fig. 2.6. A hybrid multiterminal system contains a combination of parallel and series connections of converter stations.

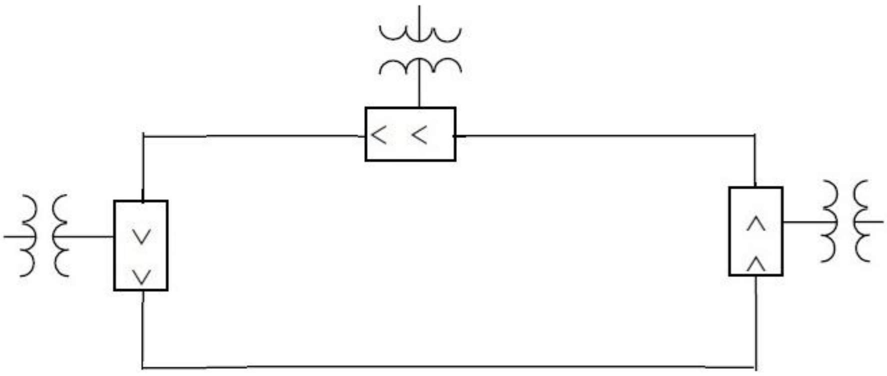

Figure 2.5: Multiterminal series link

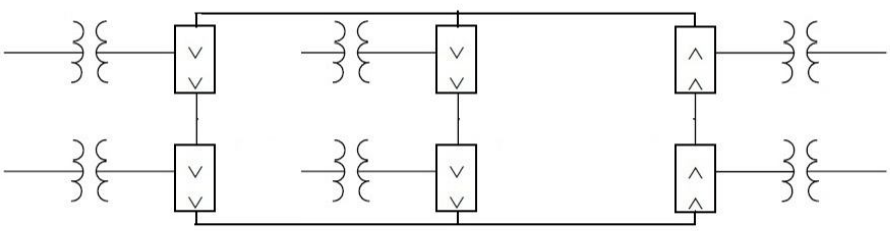

Figure 2.6: Multiterminal parallel link

2.2 Components of HVDC System

A typical HVDC system, shown in Fig. 2.7, comprises AC filters, transformers, converters, smoothing reactors, DC capacitors and DC lines/cables, Electrodes and AC circuit Breakers [5], [6].

Converters

Perform AC/DC and DC/AC conversion. The valve bridges consists of high voltage valves

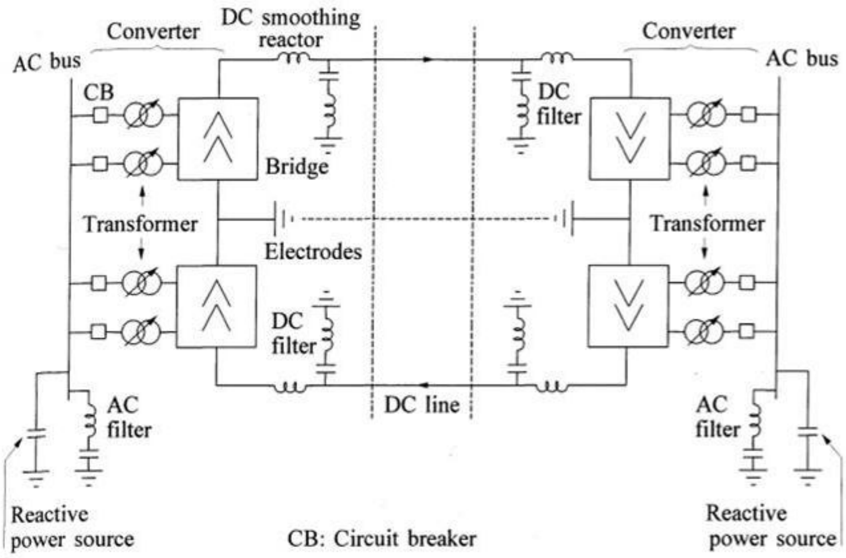

Figure 2.7: Components of HVDC system

connected in a 6-pulse or 12-pulse arrangements as shown in Fig. 2.8.

Transformers

Normally, the converters are connected to the AC system via transformers. The most important function of the transformers is to transform the voltage of the AC system to a level suitable for the converter

Smoothing reactors

These are large reactors having inductance as high as 1.0 H connected in series with each pole of each converter station which serves following purposes:

1) Decrease harmonic voltages and currents in the DC line.

2) Prevent current from being discontinuous at light load.

3) Limit the crest current in the rectifier during short-circuit on the DC line.

AC Filters

The AC voltage output contains harmonic components, caused by the switching of the Thyristirs/IGBTs. The harmonics emitted into the AC system have to be limited to prevent them from causing malfunction of AC system equipment or radio and telecommunication disturbances.

Electrodes

Most DC lines are designed to use earth as a neutral conductor for some time. The connection to the earth requires a large-surface-area conductor to minimize current densities and surface voltage gradients. This conductor is referred to as an electrode.

AC Circuit Breakers

For clearing faults in the transformer and for taking the DC line out of service, circuit-breakers are used on the AC side.

DC Lines

These may be overhead lines or cables.

2.3 Converter Performance Analysis

HVDC converter also known as Graetz bridge is shown in Fig. 2.8. Normally two such six pulse converters, one connected Y-Y and the other Y-Δ transformers are used. This helps in eliminating multiples of sixth harmonics on the dc side which reduces harmonic filters significantly.

The following assumptions are made during analysis [5].

a) All phases of the supply voltage are identical and are displaced by exactly 120^o;

b) The direct current (I_d) is constant and ripple free;

c) The transformer leakage reactance is unchanged;

d) The valves are ideal switches.

2.3.1 Operation of the bridge

Fig. 2.8 shows the bridge which consists of six thyristors (SCR) 1 to 6 that are supplied from a transformer for converting AC to DC and vice-versa. The valves fails to ignite if the delay angle exceeds 180^o. Referring to the Fig. 2.9, average direct voltage when delay angle is equal to α is given by

$$V_d = V_{do} \cos\alpha \tag{2.1}$$

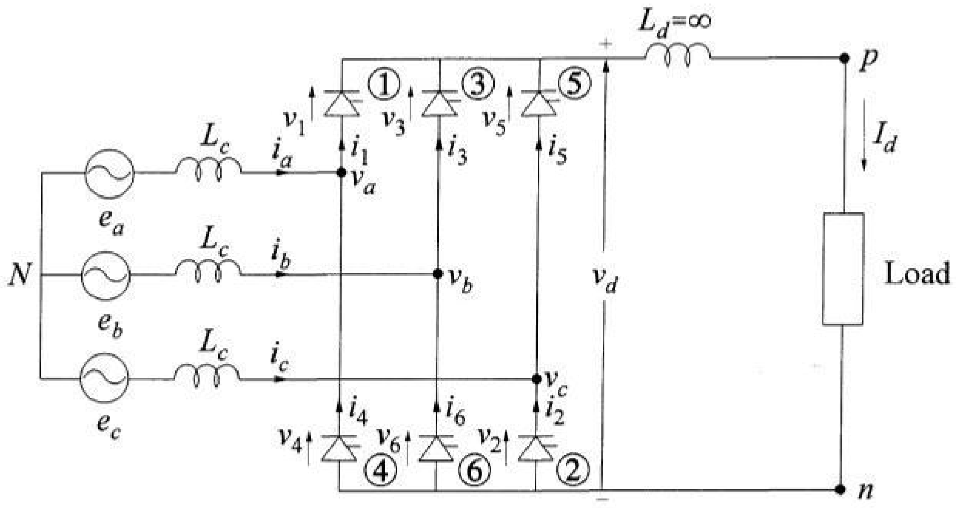

Figure 2.8: Three phase, full wave Graetz circuit

where $V_{do} = \frac{3\sqrt{2}}{\pi} E_{LL}$

Desired output voltage can be obtained by controlling firing angles *i.e* ignition delay angle for rectifier, extinction advance angle for inverter or by varying converter transformer tapings.

Due to the presence of AC source inductance, the transfer of current from one phase to another phase requires some time is called commutation time. let us consider the commutation from valve 1 to valve 3. Commutation begins at ωt=α and ends when ωt=α+μ=δ during the period of commutation

$$e_b - e_a = L_c \frac{di_3}{dt} - L_c \frac{di_3}{dt} \tag{2.2}$$

since $i_1 = I_d - i_3$

$$\frac{di_1}{dt} = 0 - \frac{di_3}{dt} \tag{2.3}$$

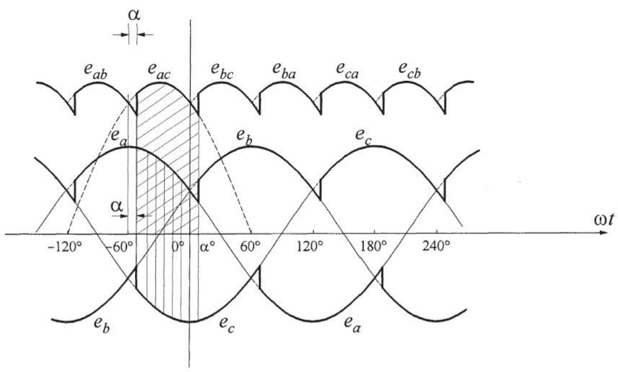

Figure 2.9: Output voltage waveforms with firing angle delay

Then

$$i_3 = \frac{\sqrt{3}E_m}{2\omega L_c}(\cos\alpha - \cos\omega t) \tag{2.4}$$

The corresponding average voltage drop is

$$\Delta V_d = \frac{V_{do}}{2}(\cos\alpha - \cos\delta) \tag{2.5}$$

from Eqn's 2.4 and 2.5

$$V_d = V_{do}\cos\alpha - R_c I_d \tag{2.6}$$

The RMS value of the fundamental frequency component of the alternating line current is [6]

$$I_1 = \frac{\sqrt{6}}{\pi} I_d \tag{2.7}$$

If we neglect losses in the converter, ac power must be equal to dc power then power factor of the fundamental wave is

$$\cos\phi = \cos\alpha \tag{2.8}$$

So, when the converter acts as a rectifier or a inverter draws reactive power from the system.

2.3.2 Rectifier operation

The equivalent circuit of the bridge rectifier based on the above analysis is shown in figure 2.10.

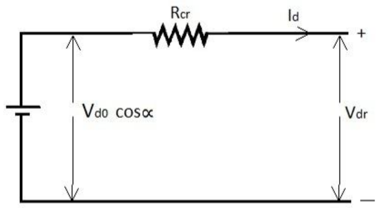

Figure 2.10: Equivalent circuit of rectifier

2.3.3 Inverter operation

As valves conducts only in one direction reversal of power takes place with reversal of direct voltage. An alternating voltage must exist on the primary side of the transformer for inverter operation. The direct voltage of the inverter opposes the current, as in a dc motor, and is called as counter voltage. The inverter operation also be described in terms of α and δ as

$\beta = \pi$-α = ignition advance angle

$\gamma = \pi$-δ = extinction advance angle

$\mu = \delta$-$\alpha = \beta$-γ = overlap

since $\cos\alpha$ = -$\cos\beta$ and $\cos\gamma$=-$\cos\delta$

The general converter equations can be written as

$$V_d = V_{do}\cos\gamma - R_c I_d \tag{2.9}$$

Figure 2.11 shows the inverter equivalent circuit

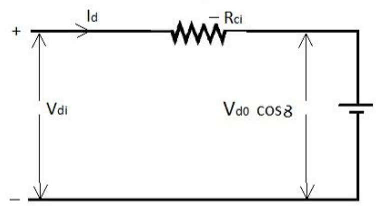

Figure 2.11: Equivalent circuit of inverter

2.4 HVDC Transmission Advantages

Following are the main advantages of HVDC transmission compared to AC transmission system [1], [2].

(1) A bipolar HVDC overhead line only requires two conductors with positive and negative polarities, thereby providing simple tower structure, low DC-line investment and less power loss. Compared to a double circuit HVAC line with six conductor bundles, one bipolar HVDC line with two conductor bundles takes much less the width of transmission routine. Under the effect of direct voltage, the capacitance of transmission line is never taken into account. Since capacitive current does not exist, direct voltage maintains the same along the transmission line.

(2) For the AC and DC cables with the same insulation thickness and cross section, the transmission capability for DC cable is considerably higher than that for AC cable. DC cable lines only require one cable for monopolar link or two cables for bipolar link and AC cable lines need three cables, due to three phase AC transmission. Therefore, the price for DC cable lines is substantially lower than AC cable lines. Since there is no the cable capacitance in a DC cable transmission, the transmission distance for DC cable is unlimited theoretically.

(3) HVDC links can be used to interconnect asynchronous AC systems and the short circuit current level for each AC system interconnected will not increase. The intercon-

nected AC systems can be operated with different nominal frequencies and the exchange power between interconnected AC systems can be controlled rapidly and accurately.

(4) Due to the rapid and controllable features, HVDC systems can be used to improve the performance of AC system, e.g. the stability of frequency and voltage, the power quality and reliability of interconnected AC systems. For the DC/AC hybrid transmission system, the rapid and controllable features of HVDC system can also be used to dampen the power oscillations in AC systems, so as to increase AC lines transmission capacity.

(5) For an HVDC system, earth can be used as the return path with lower resistance, loss and operational cost. For a bipolar link, earth is normally used as a backup conductor. If faults occur on one pole, the bipolar link can be changed into the monopolar link automatically, thereby improving the reliability of HVDC system.

(6) An HVDC transmission system can also be used to link renewable energy sources, such as wind power, when it is located far away from the consumer.

2.5 HVDC Transmission Disadvantages

Some of HVDC transmission disadvantages are,
(1) in a converter station, except for converter transformers and circuit breakers, there are converter valves, smoothing reactors, AC filters, DC filters and reactive power compensators. For the same rating, the investment for a converter station is several times higher than the investment for an AC substation.

(2) a converter acts as not only a load or a source, but also a source of harmonic currents and voltages, thereby distorting current and voltage waveforms.

(3) In a conventional converter station, the reactive power demand is approximately 60 percent of the power transmitted at full load. Since, reactive power must balance in-

stantaneously. Reactive power compensators must be installed in the converter station in order to improve the stability of commutation and dynamic voltage.

(4) without current zero crossing point, DC circuit breakers are difficult to manufacture, thereby developing multiterminal HVDC systems very slowly. With developing power semiconductors with high switching frequency, DC circuit breaker can be innovated.

2.6 HVDC Transmission Applications

The first application for HVDC converters was to provide point-to-point electrical power interconnections between asynchronous AC power networks. There are other applications which can be met by HVDC converter transmission which include [1]

Long Distance and Bulk Capacity Transmission

For the same transmission capacity, above a certain distance, an HVDC transmission offers more economic benefits than HVAC transmission. As the transmission distance increases, the transmission capacity for HVAC line is restricted by stability limitation, thereby necessarily increasing additional investment for short-circuit limitation, voltage support.

Power System Interconnection

In order to optimize the resource utilization, several AC systems intend to be interconnected with the development of power industry, but it will give rise to the problems in the super system. For example, the interconnection for AC systems always increases the short-circuit levels, thereby exceeding the capacity of the existing circuit breakers. AC systems can also be interconnected by HVDC transmission and thereby, not only obtains the interconnection benefits but also avoids the serious consequences.

DC Cable Transmission

For DC cable, without capacitance current, the transmission capacity is not restricted by transmission distance. Except for the purpose of long distance and bulk capacity, DC cables are also widely used across strait in the world. Due to environmental issue, large capacity power stations are not allowed to build in the vicinity of city. Moreover, it is very difficult to select appropriate the over headline routine, owing to high population and load density. Therefore, using HVDC underground/submarine cables is an attractive solution to deliver power from remote power station to urban load center.

Increasing the capacity of power transmission

It is some what difficult for new transmission rights of way. But, if we upgrade the existing overhead AC transmission lines with DC transmission can substantially increase the power transfer capability on the existing right of way.

2.7 Control of HVDC System

2.7.1 Basic principles of control

An HVDC transmission system is highly controllable. Its effective use depends on appropriate utilization of controllability to ensure desired performance of the power system.consider a monopolar HVDC link whose equivalent circuit is shown in Fig. 2.12. Where subscript r and i refer to rectifier and inverter respectively.
The following issues are considered
(1) The transformers have variable transforming ratios. The effect of leakage reactance on DC voltage was included through the commutation resistance R_{cr} on rectifier side and R_{ci} on inverter side.
(2) The DC overhead line is represented through resistance and its reactance is neglected.

A terminal which supplies power to DC link is termed as rectifier terminal and the

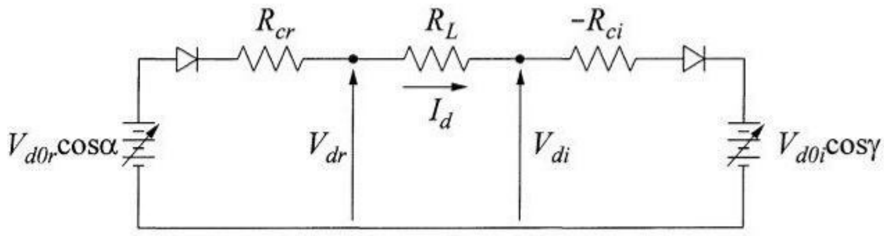

Figure 2.12: Equivalent circuit of an monopolar HVDC link

terminal which takes power from DC link is termed as inverter terminal. The direction of power flow can be changed by changing firing angle control.
The direct current flowing from the rectifier to the inverter in a monopolar HVDC link can written as

$$I_d = \frac{V_{dr} \cos\alpha - V_{di} \cos\gamma}{R_{dc}} \tag{2.10}$$

The power at the rectifier terminal is

$$P_{dr} = V_{dr} I_d \tag{2.11}$$

and at the inverter terminal

$$P_{di} = V_{di} I_d = P_{dr} - R_L I_d^2 \tag{2.12}$$

The direct voltage at any point on the line and the current can be controlled by controlling the internal voltages ($V_{dor} \cos\alpha$) and ($V_{doi} \cos\gamma$). This is accomplished by gate control of valve ignition angle or control of the ac voltage through tap changing of the converter transformer.

2.7.2 Basis for selection of controls

The following considerations influence the selection of control

1) Prevention of large fluctuations in direct current due to variations in ac system voltage.

2) Maintaining direct voltage near rated value

3) Maintaining power factors at the sending and receiving end that are as high as possible.

There are several reasons for maintaining the power factor high

(a) To reduce the stresses in the valves.

(b) To minimize losses and current rating of equipment in the ac system to which the converter is connected.

(c) To minimize voltage drops st the ac terminals as loading increases and

(d) To minimize the cost of reactive power supply to the converters.

Rapid control of the converters to prevent large fluctuations in direct current is an important requirement for satisfactory operation of the HVDC link. Referring to equation (2.10), the line resistance is small. Hence, a small change in V_{dr} or V_{di} causes a large change in I_d. It means even 25 % change in voltage at either the rectifier or inverter could cause direct current to change by as much as 100%. This implies that, if both α and γ are kept constant, the direct current can vary over a wide range for small changes in the alternating voltage magnitude at either end. Such variations are not unacceptable for satisfactory performance of the power system. In, addition to this the resulting current may be high enough to damage the valves and other equipment. Therefore, rapid converter control to prevent fluctuations of direct current is essential for proper operation of the system, without such a control the HVDC system would be impractical.

For a given power transmitted, the direct voltage profile along the line should be close to the rated value. This minimizes the direct current and thereby the line losses.

Chapter 3

Power Flow Studies

Power flow analysis aims at determination of system parameters like voltage, current, power factor and power (real and reactive) flow at various points in the electric system under existing conditions of normal operation. This analysis helps in determining the scope of future expansion of the system. Power flows studies, commonly referred to as load flow, are the backbone of power system analysis and design. They are necessary for planning, operation, economic scheduling and exchange of power between utilities. In addition, power flow analysis is required for many other analyses such as transient stability and contingency studies.

3.1 Significance of Load Flow Study

1. Determination of current, voltage, voltage angle, active power, reactive power etc. at various buses in power system operating under normal steady state or static condition.

2. To plan best operation and control of existing system.

3. To plan future expansion to keep pace with load growth.

4. Help in ascertaining the effect of new load, new generating stations, new lines and

new interconnections before they are installed.

5. Due to this information system losses are minimized and also check is provided on system stability.

6. Provides the proper prefault power system analysis to avoid system outage due to fault.

3.2 Types of Buses

Four variables are associated with each node

a. Bus voltage magnitude (V)

b. Voltage angle (δ)

c. Real power (P)

d. Reactive power (Q)

Each node introduces two equations, namely the real and reactive power balance equations. To obtain solutions for a set of simultaneous equations, it is necessary to have the same number of equations as unknowns. Therefore two of the variables associated with each bus must be specified. The other two variables are free to vary during the solution process. The traditional way of specifying bus-bar quantities allows buses to be identified as follows

3.2.1 PQ bus-bar

At which the net active and reactive powers are specified. The net power entering a bus-bar is the power supplied to the system from a generating source minus the power consumed by a load at that bus-bar.

3.2.2 PV bus-bar

At which the net active power is specified, and the voltage magnitude is specified. The net reactive power is an unknown which is determined as part of the power flow solution.

This type of bus-bar typically represents a node in the system at which a synchronous source (generator or compensator) is connected, where the sources reactive power output is varied to control the voltage magnitude to a scheduled value.

3.2.3 Slack or swing bus-bar

Where the voltage magnitude and angle are specified. Generally the angle is set to zero. Unlike the other two bus types, which represent physical system conditions, this bus-bar type is more a mathematical requirement. It is needed to provide a reference angle to which all other angles are referred. Also, this bus absorbs any real power mismatch across the system. Normally there can only be one slack bus-bar in the system. It is generally chosen from among the voltage controlled bus-bars.

3.3 Formulation of Power Flow by Newton-Raphson Method

Consider an n -bus power system contains a total np number of P-Q (load) buses while the number of P-V (generator) buses be ng such that n = np + ng + 1. Bus-1 is assumed to be the slack bus. The approach to Newton-Raphson load flow is similar to that of solving a system of nonlinear equations using the Newton-Raphson method. At each iteration formation of Jacobian matrix and solve for the corrections are given in Eq'n 3.1. For the load flow problem, this equation is of the form

$$\begin{bmatrix} J \end{bmatrix} \begin{bmatrix} \Delta\delta_2 \\ . \\ . \\ \Delta\delta_n \\ \frac{\Delta V_2}{|V_2|} \\ . \\ . \\ \frac{\Delta V_n}{|V_n|} \end{bmatrix} = \begin{bmatrix} \Delta P_2 \\ . \\ . \\ \Delta P_n \\ \Delta Q_2 \\ . \\ . \\ \Delta Q_{np} \end{bmatrix} \tag{3.1}$$

Where

Real and Reactive power injections at each bus is given by

$$P_i = |V_i|^2 G_{ii} + \sum_{k=1,k\neq i}^{n} |Y_{ik} V_i V_k| \cos(\theta_{ik} + \delta_k - \delta_i) \tag{3.2}$$

$$Q_i = -|V_i|^2 B_{ii} - \sum_{k=1,k\neq i}^{n} |Y_{ik} V_i V_k| \sin(\theta_{ik} + \delta_k - \delta_i) \tag{3.3}$$

and Jacobian matrix is divided into submatrices as

$$\begin{bmatrix} J \end{bmatrix} = \begin{bmatrix} J_{11} & J_{12} \\ J_{21} & J_{22} \end{bmatrix} \tag{3.4}$$

The size of the jacobian matrix will be (n+n_p-1) × (n+n_p-1) and the submatrices are

$$J_{11} = \begin{bmatrix} \frac{\partial P_2}{\partial \delta_2} & . & . & \frac{\partial P_2}{\partial \delta_n} \\ . & . & & . \\ . & & . & . \\ \frac{\partial P_n}{\partial \delta_2} & . & . & \frac{\partial P_n}{\partial \delta_n} \end{bmatrix} \tag{3.5}$$

$$J_{12} = \begin{bmatrix} |V_2|\frac{\partial P_2}{|V_2|} & . & . & |V_{1+np}|\frac{\partial P_2}{|V_{1+np}|} \\ . & . & & . \\ . & & . & . \\ |V_2|\frac{\partial P_n}{|V_2|} & . & . & |V_{1+np}|\frac{\partial P_n}{|V_{1+np}|} \end{bmatrix} \tag{3.6}$$

$$J_{21} = \begin{bmatrix} |V_2|\frac{\partial Q_2}{|V_2|} & . & . & |V_{1+np}|\frac{\partial Q_2}{|V_{1+np}|} \\ . & . & & . \\ . & & . & . \\ |V_2|\frac{\partial Q_n}{|V_2|} & . & . & |V_{1+np}|\frac{\partial Q_n}{|V_{1+np}|} \end{bmatrix} \tag{3.7}$$

$$J_{22} = \begin{bmatrix} \frac{\partial Q_2}{\partial \delta_2} & . & . & \frac{\partial Q_2}{\partial \delta_n} \\ . & & . & . \\ . & & . & . \\ \frac{\partial Q_{1+np}}{\partial \delta_2} & . & . & \frac{\partial Q_{1+np}}{\partial \delta_n} \end{bmatrix} \tag{3.8}$$

and Newton-Raphson procedure is as follows

Step-1: Choose the initial values of the voltage magnitudes $|V|^{(0)}$ of all np load buses and n-1 angles $\delta^{(0)}$ of the voltages of all the buses except the slack bus.

Step-2: Use the estimated $|V|^{(0)}$ and $\delta^{(0)}$ to calculate a total n-1 number of injected real power $Pcalc^{(0)}$ and equal number of real power mismatch $\Delta P^{(0)}$.

Step-3: Use the estimated $|V|^{(0)}$ and $\delta^{(0)}$ to calculate a total np number of injected reactive power $Qcalc^{(0)}$ and equal number of reactive power mismatch $\Delta Q^{(0)}$.

Step-3: Use the estimated $|V|^{(0)}$ and $\delta^{(0)}$ to formulate the Jacobian matrix $J^{(0)}$.

Step-4: Solve (4.30) for $\delta^{(0)}$ and $\frac{\Delta V^{(0)}}{|V^{(0)}|}$.

Step-5: Update the voltage magnitudes and voltage angles from

$$\delta^{(1)} = \delta^{(0)} + \Delta\delta^{(0)}$$

$$|V|^{(1)} = |V|^{(0)}[1 + \frac{\Delta|V|^{(0)}}{|V|^{(0)}}]$$

Step-6: Check if all the mismatches are below a small number. Terminate the process if yes. Otherwise go back to step-1 to start the next iteration with the updated values obtained from step-5.

3.4 AC-DC Power Flow

Most of the solution techniques for AC/DC power flow are divided into two different approaches [10], [11], [12]. The sequential and the unified (or simultaneous) solution methods. The sequential solution methods, AC and DC system equations are solved separately in each iteration until the terminal conditions of converters are satisfied. Because of modular programming, the sequential methods are generally easy to implement and simple to incorporate various control specifications. In the unified methods, the AC as well as DC system equations are combined together with the residual equations, describing the rectifier terminal behaviors, in one set of equations to be solved simultaneously. The unified methods, with their better computing efficiency and convergence, seem more suitable than the sequential methods for use in industrial AC/DC power systems, even if they might be more complicated to program.

The Gauss-Seidel (G-S), the Newton-Raphson (N-R), and the fast decoupled N-R methods may be used to solve the power flow problems in AC/DC systems as they do in the pure AC systems. The G-S method generally needs accelerating factors to improve the iteration process because of its slow rate of convergence. The N-R method, with its powerful convergence characteristics, appears to be the most attractive technique in solving the AC/DC power flows.

3.4.1 Point-to-point HVDC

When the AC system includes a HVDC link, say rectifier is connected at bus *fr* and inverter is connected at bus *to* with transformer taps of $1{:}t_1$ and $1{:}t_2$. Then the operating condition of a an AC-DC power system is defined by the vector

$$[\bar{V}, \bar{\theta}, \bar{x}]^T \tag{3.9}$$

Where

$\bar{V}$ is a vector of the voltages magnitudes at all AC system busbars

$\bar{\theta}$ is a vector of the angles at all AC system busbars (except the reference bus which is assigned $\theta = 0$)

$\bar{x}$ is a vector of DC variables

The equations of power balance at the terminal buses of the AC system are modified by including the powers at the converter stations *i.e.*, at rectifier end both active and reactive powers are consumed and at the inverter end real power is injected and reactive power is consumed [11], [12].

Then power mismatches at AC-DC buses are

$$\Delta P_{fr} = P_{G,fr} - P_{L,fr} - P_{dc,fr} \tag{3.10}$$

$$\Delta P_{to} = P_{G,to} - P_{L,to} + P_{dc,to} \tag{3.11}$$

$$\Delta Q_{fr} = Q_{G,fr} - Q_{L,fr} - Q_{dc,fr} \tag{3.12}$$

$$\Delta Q_{to} = Q_{G,to} - Q_{L,to} - Q_{dc,to} \tag{3.13}$$

where

P_G , Q_G are function of AC system variables

P_L , Q_L are usual AC system load at bus

P_{dc} , Q_{dc} are function of DC system variables as

$$P_{dc} = f(V_{dr}, V_{di}, \bar{x}) \tag{3.14}$$

$$Q_{dc} = f(V_{dr}, V_{di}, \bar{x}) \tag{3.15}$$

where

V_{dr},V_{di} are the voltage magnitudes at the rectifier and inverter buses;

$\bar{x}$ is the vector of independent variables of the HVDC system.

Because of introduction of the vector of unknowns $\bar{x}$, supplementary equations describing the DC link operation and control strategy should be added as

$$R(V_{dr}, V_{di}, \bar{x}) = 0 \tag{3.16}$$

So, the non linear system of equations use in the load flow calculation of mixed AC DC system by using the extended variables method are

$$\begin{pmatrix} \Delta P(\bar{V}, \bar{\theta}) \\ \Delta P(\bar{V}, \bar{\theta}, [\bar{x}]) \\ \Delta Q(\bar{V}, \bar{\theta}) \\ \Delta Q(\bar{V}, \bar{\theta}, [\bar{x}]) \\ R(V_{dr}, V_{di}, \bar{x}) \end{pmatrix} = 0 \tag{3.17}$$

(A) At rectifier side

1) The DC voltage in terms of the AC source voltages referred to the transformer secondary is

$$V_{dr} = \frac{3\sqrt{2}}{\pi} t_1 V_{fr} \cos\alpha \tag{3.18}$$

where V_{fr} is the busbar voltage on the system side of the converter transformer and α is the gating delay for rectifier operation

2) Current flowing through the line is same as Eq'n 2.6.

3)The primary current drawn by the transformer at rectifier end is given by

$$I_1 = \frac{\sqrt{6}}{\pi} t_1 I_d \tag{3.19}$$

4)If we assume converter transformer is lossless and the magnetising admittance is ignored, then the primary real power consumed by rectifier can be written as

$$P_{dr} = V_d.I_d = V_{fr} I_1 \cos\alpha \tag{3.20}$$

5) Reactive power consumed consumed can be written as

$$Q_{dr} = V_{fr} t_1 I_1 \sin\alpha \tag{3.21}$$

The DC variables are

$$[\bar{x}] = [V_{dr}, I_d, t_1, \cos\alpha]^t \tag{3.22}$$

$\cos\alpha$ is used as a variable than α is to linearize the equations.

(B) At inverter side

The equations presented above are equally applicable to inverter operation. But, during inversion extinction advance angle γ controls the action instead of ignition delay angle α. Therefore, DC voltage after inversion is

$$V_{di} = \frac{3\sqrt{2}}{\pi} t_2 V_{to} \cos\gamma \tag{3.23}$$

(C) DC per unit base

Computational simplicity can be achieved by using common power and voltage base parameters on both sides of the converter. But to maintain consistency of power in per unit the direct current base is $\sqrt{3}$ times more than the AC current base as

$$I_1 = \frac{\sqrt{6}}{\pi} I_d \tag{3.24}$$

Translating above equation to per unit yields

$$I_1(p.u.) = \frac{\sqrt{6}}{\pi} \sqrt{3} I_d(p.u.) \tag{3.25}$$

(D) Incorporation of control equations

In a AC - DC hybrid system, DC link operating condition is determined by means of the values of the electrical quantities associated to the converter station which are grouped into a vector

$$[X] = [V_{dr}, t_1, \cos\alpha, V_{di}, t_2, \cos\gamma, I_d]^t \tag{3.26}$$

As we have three equations like at the rectifier, at the inverter, the DC line configuration and seven independent variables. So, four more equations are to be added for modeling the control strategy of the DC link by specifying the four independent variables and also the limit values (minimum and maximum limits) and thus the operating mode is obtained. Examples of valid control specifications are

(i) Specified converter transformer tap

$$t - t^{sp} = 0 \tag{3.27}$$

(ii) Specified DC voltage

$$V_d - V^{sp} = 0 \tag{3.28}$$

(iii) Specified minimum firing angle

$$\cos\alpha - \cos\alpha^{sp} = 0 \tag{3.29}$$

(iv) Specified DC power transmission

$$V_d I_d - P_{DC}^{sp} = 0 \tag{3.30}$$

Above control equations are simple and are easily incorporated into the solution algorithm. During the iterative solution procedure the uncontrolled converter variables may go outside (minimum or maximum limit) pre-specified limits. When this occurs the offending variable is usually held to its value equal to the exceeding limit and then next operating mode is considered. Thus, Some of the operating modes are [12], [14]

(1) $\cos\alpha$ P_{di} $\cos\gamma$ V_{di}

(2) $\cos\alpha$	P_{di}	t_2	V_{di}
(3) t_1	P_{di}	t_2	V_{di}
(4) t_1	P_{di}	$\cos\gamma$	V_{di}
(5) t_1	P_{di}	$\cos\gamma$	t_2
(6) t_1	P_{di}	$\cos\alpha$	$\cos\gamma$
(7) t_1	V_{dr}	$\cos\gamma$	P_{di}

Some more control modes can be obtained,

(A) if the current I_d is kept constant instead power P_{di} ;

(B) by keeping constant power P_{dr} instead of P_{di};

(C) if the voltage at rectifier side i.e., V_{dr} in place of V_{di}

The operating mode one corresponds to operation with constant angles α and γ, ensured by transformer tap changers in order to maintain constant power and voltage desired through DC line. Suppose, in this process if the transformer tap positions hits the maximum or minimum limits then the tap changer variable will be fixed to the exceeded limit and the operating mode of DC link will now shift to mode two or four depending on the variable which is exceeded. Thus continuous operation of DC can be obtained.

Rectifier, has a minimum α limit of about 5^o to ensure adequate voltage across the valve before firing and it is normally operates at a value of α within the range of 15^o to 30^o so as to leave some room for increasing rectifier voltage to control DC power flow [7].

In case of an inverter, it is necessary to maintain a certain minimum extinction angle [7] to avoid commutation failure. It is important to ensure that commutation is completed with sufficient margin to allow for de-ionization before commutating voltage reverse at $\alpha = 180^o$ or $\gamma = 0^o$. The extinction angle γ is equal to $\beta - \mu$ with overlap μ depending on I_d and the commutating voltage. Since a converter transformer has inductance, the transformer current cannot change instantly. The finite rate of change of current means that the transfer of current from one valve to another requires a finite commutation time. The volttime area A, which is shown in Figures 3.1 and 3.2. is required for the commutation. The volt-time area A is related to the commutating current. The higher the commutating current, the larger the volt-time area A will be. Typical full load values of μ are in the range 20^0 to 50^0 under normal steady-state operation.

Commutation failures in HVDC systems are mainly caused by voltage dips due to AC system faults. As indicated in Fig. 3.1 and Fig 3.2, voltage dips may cause both voltage magnitude reduction and phase-angle shift [8]. Voltage dips may affect the commutation in three ways:

1) **Voltage magnitude reduction**

Commutating ac line-to-line voltage decreases because of a voltage dip, as shown in Fig.(b) in Fig. 3.1. Since the voltage magnitude has decreased, but the commutation area still remain the same, so the end of commutation will be delayed and the extinction angle will change from γ to $\acute{\gamma}$.

2) **Phase-angle shift**

The classification of three-phase voltage dips is shown in Fig.(a) in Fig. 3.1. Figure shows that the phase-angle of the line-to-line voltage may shift either backward or forward during voltage dips. The backward phase-angle shift affects the commutating process negatively. If we assume that the firing instant does not change, although the volt-time area remains the same, the final extinction is reduced from γ to $\acute{\gamma}$.

3) **Increased dc current.**

The dc current increases on the initiation of the fault at the inverter. Since the volt-time area increases with the increased dc current, a relatively larger overlap μ will be needed to complete the commutation. This will in the end reduce γ to $\acute{\gamma}$ in Fig.(c) in Fig. 3.2.

3.4.2 Multiterminal HVDC

It is increasingly being realized that multiterminal DC (MT HVDC) [15], [16] systems may be more attractive in many cases to fully exploit the economic and technical advantages of HVDC technology. When the power is to be transmitted from a large hydroelectric power station to a distant load center, if the the overhead line passes through areas whose rising

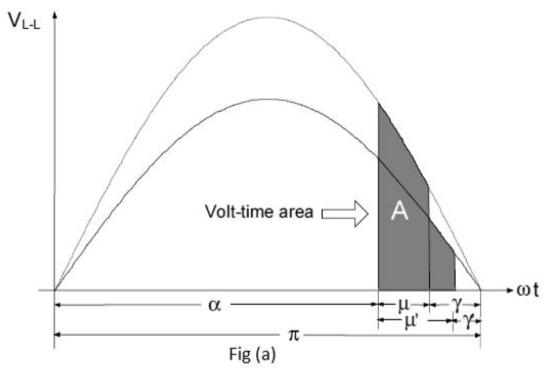

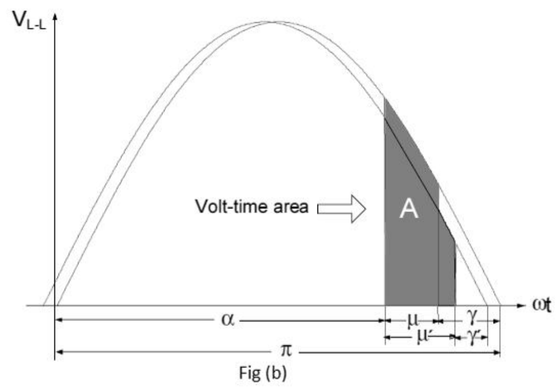

Figure 3.1: Commutation failures due to voltage magnitude reduction and phase angle shift

power demands could also be met by the new power station, then it can be solved by arranging an HVDC converter station in series or parallel in path of the dc line. In some cases combination of both series and parallel is used. It is also flexible to connect more than two power stations. Consider an example of connecting four ac networks A through D In comparison with separate HVDC point-to-point system, the HVDC multiterminal network has the following basic advantages.

(1) The number of HVDC converter stations is lower.

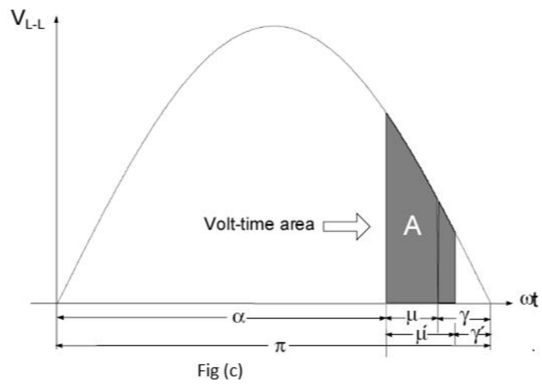

Figure 3.2: Commutation failure due to increased in DC current

enter

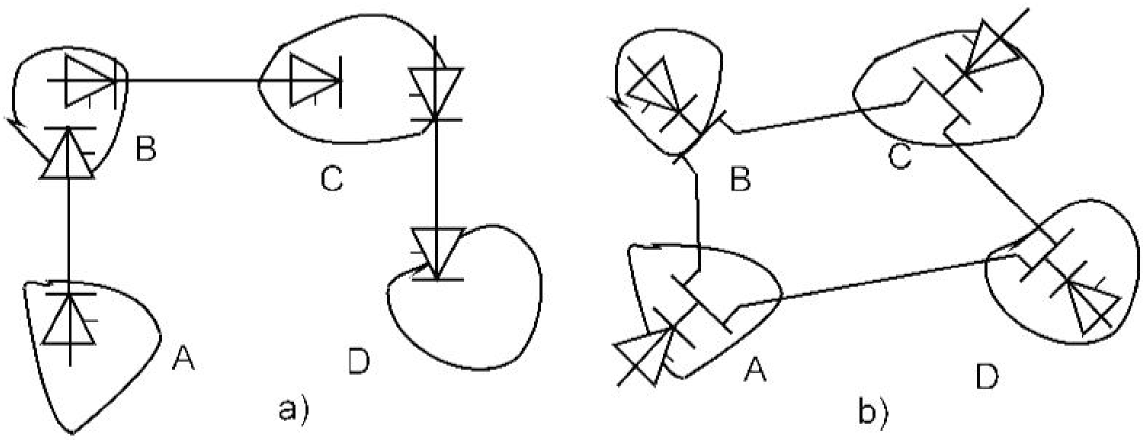

Figure 3.3: HVDC connections of several networks (a) By separate point-to-point HVDC's (b) By multiterminal HVDC
enter

(2) Transmission losses are lower since energy transport over more than two HVDC stations in series is avoided i.e., In case (a) in Fig. 3.3, the energy flow would take place from A to D through six stations.
(3) In a mesh network (additional line from A to D), a current distribution is automatically realized in the HVDC network which corresponds to minimal line losses.

In series connected multiterminal HVDC scheme, the converters are connected in series with a common direct current through all terminals. An auxiliary set up is required during start-up. One disadvantage of this is that full I^2R loss even at light load and disadvantage can be somewhat overcome by decreasing the current instead of the voltage in periods when all stations are at light load. Moreover, sometimes some converters may be light loaded and others heavily loaded, the lightly loaded converters operate at low voltage, which can be obtained either by low transformer tap or by operating at a large control angle (α or γ). The first method requires a wide tap range, which increases the cost of the converter transformer. The second method subjects the valves to large voltage jumps, which increase the probability of converter faults, increase the losses in the valve damping circuits, and increase the consumption of reactive power. This scheme is confined to applications with small power taps where it may be more economical to operate at higher current and lower voltage than for a full voltage tap at full voltage and reduced current.

On the other side parallel connected multiterminal HVDC scheme, converters are connected in parallel and operate at a common voltage is shown in Fig. 3.4 [16]. having three terminals - one rectifier and two inverters is assumed. Rectifier currents are taken as positive and inverter currents are taken as negative. The stations having the lowest ceiling voltage , *i.e.,* the lowest $V_{di} \cos \gamma_o$ controls the line voltage. This station is normally one of the inverters operating at constant extinction angle. The other two stations operate on constant current and at a voltages lower than the respective ceiling voltages.

If any of the converter is to be changed from a rectifier to an inverter or vice versa. Its current must be brought back to zero, a reverse switching must operate. Finally, the current must be increased to the desired value. This scheme is widely accepted compared to series connected scheme.

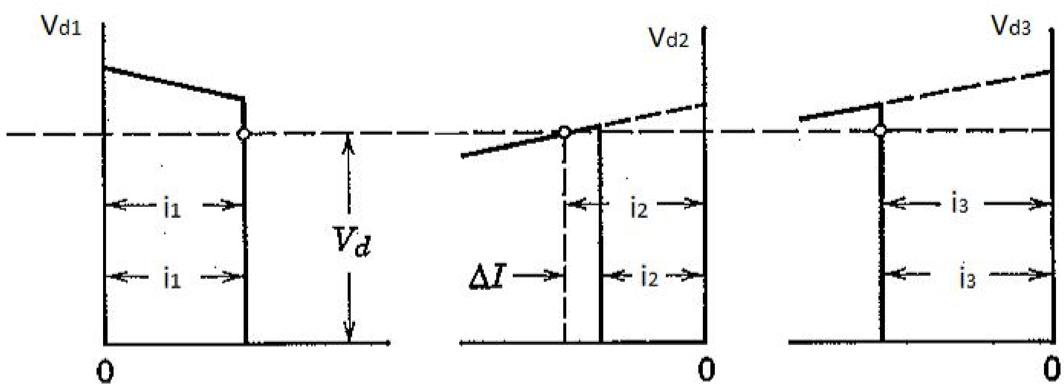

Figure 3.4: Characteristics of multiterminal parallel DC lines

(A) Power flow equations

The formulation of power flow equations developed in point-to-point connection can be easily extended to multiterminal also by simply adding network configuration equation, rectifier and inverter equations.

3.5 Results and Discussions

3.5.1 Point-to-point DC transmission Line

A four bus AC system shown in Fig. 3.5 is modified to include a DC line between buses 2 and 4. The converters at bus 2 and bus 4 operate in the rectifier mode and in the inverter mode respectively. The DC link data considered for simulation is given in Table 3.1.

$*$ = intial value for power flow iteration.

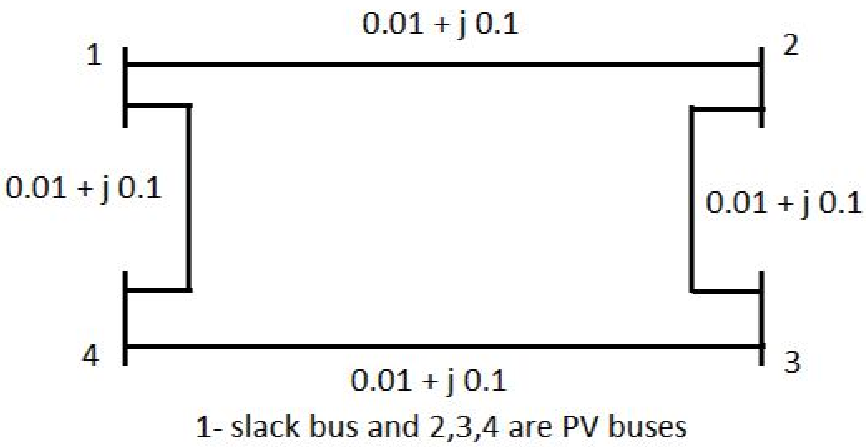

Figure 3.5: Four bus system for AC-DC load flow

Table 3.1: Converter Data

	Rectifier	Inverter
Bus Number	2	4
Minimum control angle	$\alpha_{min} = 5^o$	$\gamma_{min} = 5^o$
Resistance of the DC line	0.3	
Rated DC volatge(pu)	1.00*	1.00*
Tap of transformer	0.5*	0.5*

The number of possible modes in which HVDC can be operated are presented in Chapter 3.

The MATLAB simulation are carried out for Newton-Raphson AC-DC load flow, as explained in Section 3.4 for the case of single DC line and multiple DC lines. Lower limit on firing angles of converters is taken as 5^0. The lower and upper limits of transformer tap positions located at converters are taken as 0.7 p.u and 1.2 p.u for point-to-point. MATLAB code is written in such a way that it takes the priority of the transition modes. Transition from one mode to another mode takes place when any unspecified variable exceeds its limits. In the case of, unspecified variable exceeds its boundary limits it is fixed to the exceeded limit and one of the specified variable is freed to vary. Hence, HVDC link operating mode will be shifted to new mode provided which is specified in the priority.

Study Case (i):

Generally, for the sake of minimum reactive power requirement by the converters, converters operate at minimum firing angles. with starting mode of specifying α at rectifier, γ at inverter, for a fixed D.C voltage (V_{di}) and specified power (P_{di}) at inverter side. The simulation results, as shown in Fig. 3.6 indicates requirement of reactive power at rectifier side, inverter side and direct current flowing through D.C line. From the Fig 3.6. it is clear that the power at inverter side varying 0.8 p.u to 2.3 p.u.

It is observed from simulations results that the tap position at rectifier side exceeds its maximum limit when D.C line power is reached to 1.6 p.u. Here, the transition taken place by keeping the rectifier tap changer position at its maximum limit and the variable α is freed. The variables, t_{1max}, γ, V_{di}, P_{di}, that are going to be fixed in new operating mode after transition. In this mode firing angle, α is varied to deliver the required power at inverter side. The second transition takes place when α reached its minimum value for a power of 1.8 p.u. As depicted in Fig. 3.6, current through the DC line and reactive power is abruptly changed to large value when the second transition occurs at a power of 1.8 p.u. Hence, it could be better to operate the DC link in either first mode or second mode for specified power of the inverter.

Study Case (ii):

Instead of P_{di} in case (i), simulations are carried out by specifying power at rectifier end.

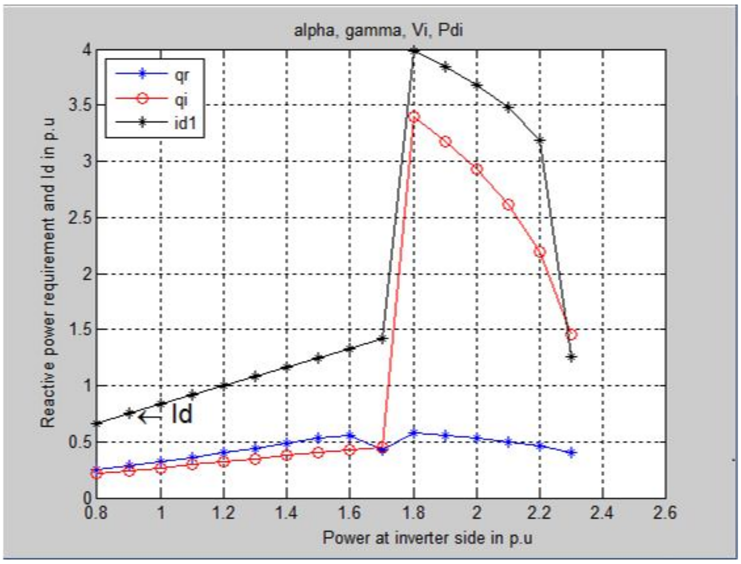

Figure 3.6: Relation between reactive power at converters, I_d versus power at inverter side in case study case (i)

From Fig.3.7, it is inferred that reactive powers consumed at the converter stations, I_d are less in this case. Same thing is also observed for the following operating modes

i) α, γ, t_1, P_{di};

ii) α, γ, t_2, P_{di};

iii) α, γ, t_1, P_{dr};

iv) α, γ, t_2, P_{dr};

But the specified tap position in the above modes influence the peak value of the direct current. Fig. 3.8 shows the reactive power values and line current for mode specifying α, γ, t2= 0.8, P_{di}. From this Fig. 3.8 it can be observed that peak value of the current is more than the current in Fig. 3.7.

Study Case (iii):

There are some combinations of variables or modes for which the operation of the DC link is difficult. For example, In mode α, $t1$, V_i and P_{di}, guessing a correct initial specified

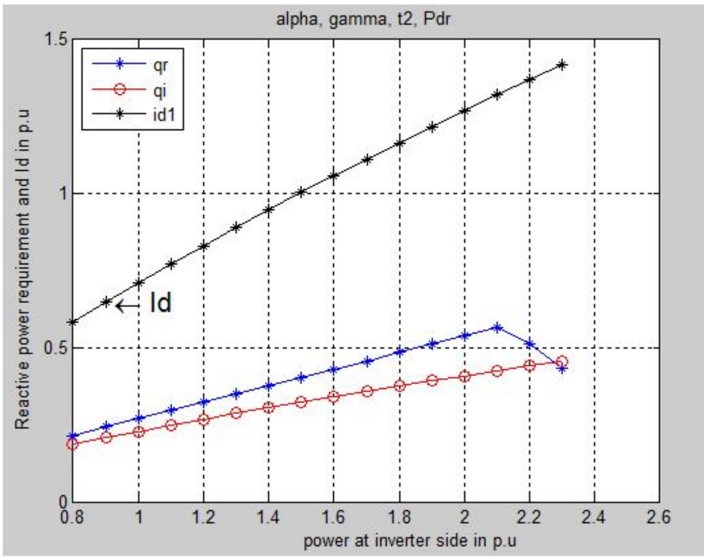

Figure 3.7: Relation between reactive power at converters, I_d versus power at inverter side in case study (ii)

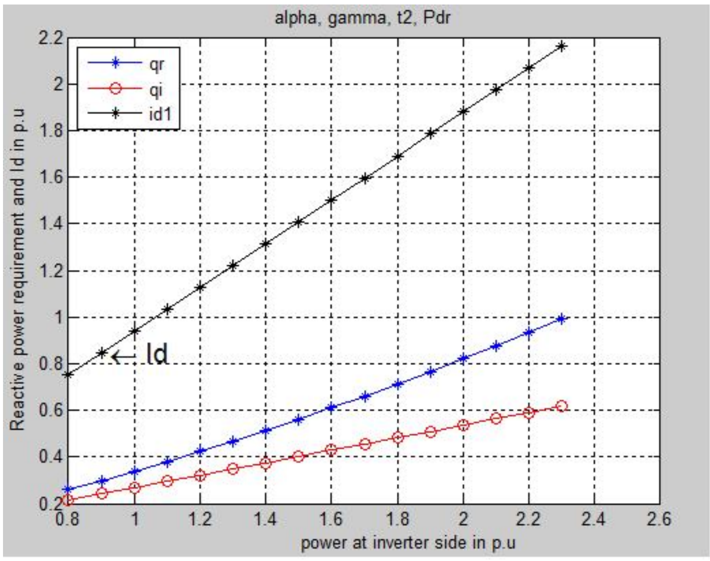

Figure 3.8: Relation between reactive power at converters, I_d versus power at inverter side in study case (iii)

values of alpha (α) and t_1 is difficult to satisfy both Eqn's 3.31 and 3.32 simultaneously.

$$I_d = \frac{V_r - V_i}{R_{dc}} \tag{3.31}$$

$$I_d = \frac{P_{di}}{V_i} \tag{3.32}$$

examples of such combinations are

i) t_1, V_r, V_i, P_{di}/P_{dr};

ii) α, t_1, V_i, P_{di}/P_{dr};

iii) γ, V_r, V_i, P_{di}/P_{dr};

iv) γ, t_2, V_r, P_{di}/P_{dr};

v) t_2, V_r, V_i, P_{di}/P_{dr};

3.5.2 Multiterminal HVDC

Multiterminal series connection

The schematic diagram for series connection of DC lines is shown in Fig. 3.9. Fig. 3.9 shows that converters Rec, Inv, Inv1, Inv2 constitutes a series connection of multiterminal HVDC. Simulations for series connection of multiterminal HVDC are shown in Fig. 3.10.

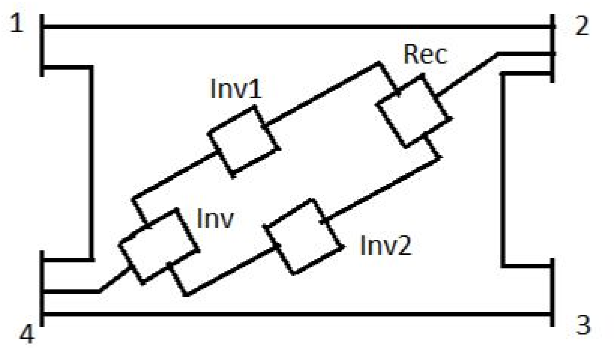

Figure 3.9: Schematic diagram of series connection

It shows the relation between tap positions of converter transformers and direct current through the line for varying power at inverter one. From the Fig. 3.10, it is found that,

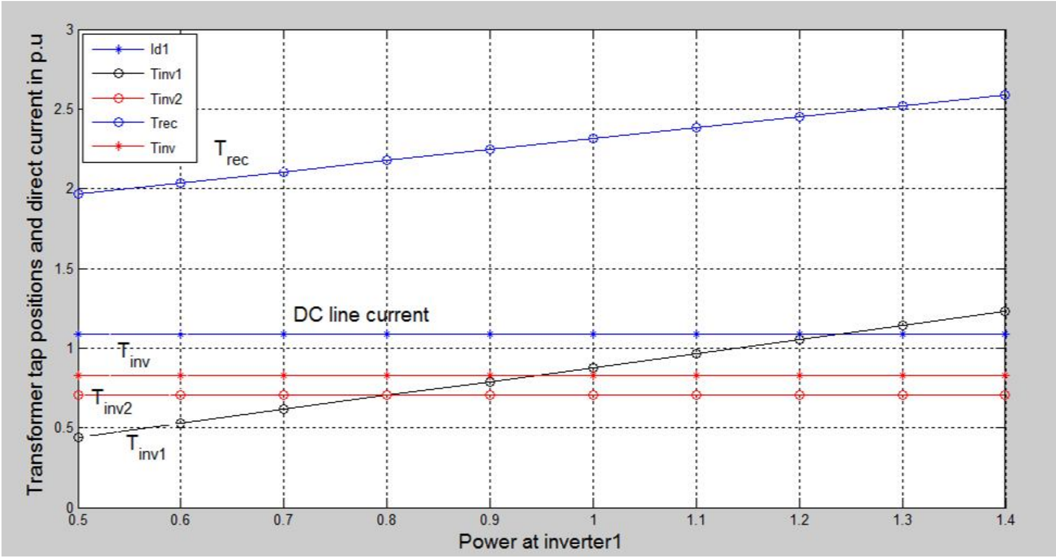

Figure 3.10: Relation between transformer tap positions at converters, I_d and power at inverter side in series connection

1) The current flowing through line is constant.

2) As the demand at inverters one is varying, tap position of transformer is also adjusted accordingly to meet the demand and the tap positions of inverter and inverter two are constant.

3)As the rectifier has to supply the sum of loads at inverters, large change in tap positions are needed which in turn increase the cost of the transformers. Because of this, series type multiterminal connection is preferred only for tapping of low power and this problem can be eliminated using radial type connection.

Multiterminal radial connection

Converters Rec1, Rec2, Inv1, Inv2 in Fig. 3.11 constitutes a radial connection of multiterminal HVDC. Converters Rec1 and Rec2 are included at buses 2 and 4 respectively.

In the simulations two multiterminal HVDC configurations *i.e.,* series and radial con-

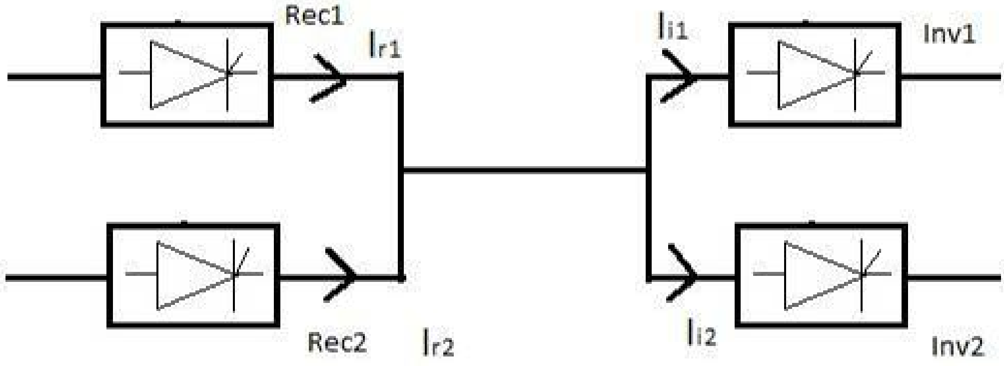

Figure 3.11: Schematic diagram of radial connection

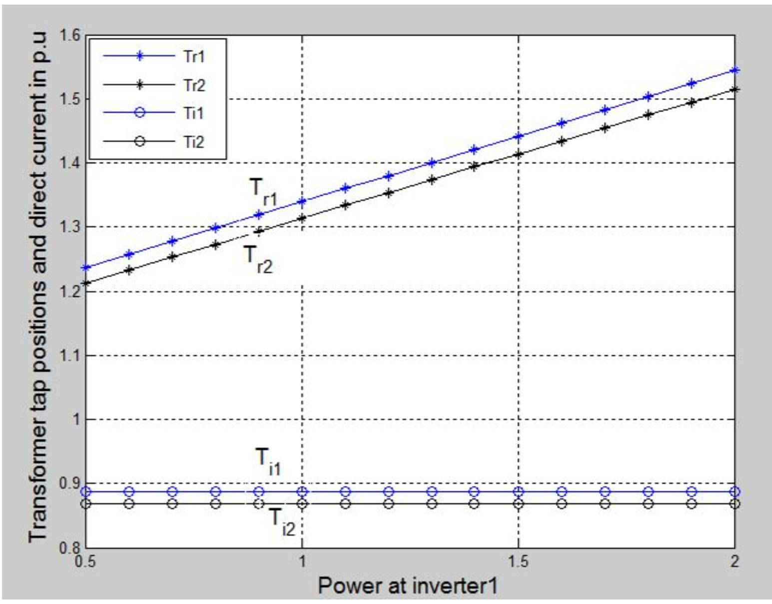

Figure 3.12: Relation between transformer tap positions at converters, I_d and power at inverter side in radial connection

nections are studied. From the simulation shown in Fig. 3.12, point out that the affect of the configurations on the taps of the transformer and in turn the effect of on the cost of the transformer.

From Fig. 3.12, it clearly indicate that for the radial configuration the range of the taps required on the transformer is less than in case of the series configuration. In both cases the load variation are kept same. So, this indicates that the case discussed, the cost of transformer is more for series configuration than the radial configuration.

Chapter 4

Optimization of Power Flow

The optimal Power Flow (OPF) problem is a powerful tool for power system operation and planning. In general, OPF problem is a nonlinear programming (NLP) problem that is used to determine the "optimal" control parameter settings to minimize a desired objective function, subject to certain system constraints. The OPF problem represents a variety of optimization problems include fuel or active power cost optimization, active power loss minimization, maximum transfer capability, MVAR cost minimization, minimum of total emission.

4.1 Conventional Optimal Economic Scheduling

Conventional optimal economic scheduling (Economic Load Dispatch activity) [19] is executed in the dispatch stage. Its primary function involves allocating the total load between the available generating units in such a way that the total cost of operation is kept at minimum. Total cost may be approximated by a variety of expressions such as linear or quadratic functions of the active power generation of the unit. The total active power generation in the system must equal the load plus the active transmission losses.

The objective function is augmented by the constraints using a Lagrange-type multiplier lambda, λ.

$$\frac{\partial F_i}{\partial P_i} = \lambda \left[1 - \tfrac{\partial P_L}{\partial P_i}\right] i = 1, ..., N$$

When the generator's limits are not binding, The optimal solution to the ELD problem is obtained when all units operate at the same value of λ *i.e.,* equal incrementing cost operation yields the optimal dispatch. The optimality conditions along with the physical constraints are a set of nonlinear equations that requires iterative methods to solve. Newtons method has been widely accepted to solve problems such as the load flow and optimal load flow.

A solution can usually be obtained within a few iterations, provided that a reasonably good initial estimate of the solution is available.

4.2 Formulation of OPF problem

In the Economic Load Dispatch(ELD), The demand is considered to be an aggregate parameter for the entire system. When load flow equations are introduced in ELD as a system of demand supply balance constraints, the optimum solution yields a set of decision variables satisfying the physical laws of flow of electricity while achieving a desired objective (of cost minimization, loss minimization ....) such a formulation is called optimal power flow (OPF). It is a static, constrained, nonlinear, optimization problem. Due to the presence of the detailed network configuration instead of lumped formulation of ELD, The demand is now disaggregated and is available at all buses individually. As the load flow equations include a reactive power balance at each node. The OPF has the additional advantage of considering reactive power as a decision variable, this leads to reactive power planning problem. The optimal power flow is a constrained optimization problem requiring the minimization of [20], [21]

$$f = (x, u) \tag{4.1}$$

subject to

$$g(x, u) = 0 \tag{4.2}$$

$$h(x, u) \leq 0 \tag{4.3}$$

$$u^{min} \leq u \leq u^{max} \tag{4.4}$$

$$x^{min} \leq x \leq x^{max} \tag{4.5}$$

Here, $f(x,u)$ is the scalar objective function, $g(x,u)$ represents nonlinear equality constraints (power flow equations), and $h(x,u)$ is the nonlinear inequality constraint of vector arguments x and u. The vector x contains dependent variables consisting of bus voltage magnitudes and phase angles, as well as the MVAr output of generators designated for bus voltage control and fixed parameters such as the reference bus angle, noncontrolled generator MW and MVAr outputs, noncontrolled MW and MVAr loads, fixed bus voltages, line parameters, etc. The vector u consists of control variables including real and reactive power generation, phase shifter angles, DC transmission line flows, control voltage settings.

The power system consists of a total of N buses, N_G of which are generator buses. M buses are voltage controlled, including both generator buses and buses at which the voltages are to be held constant. The voltages at the remaining (N - M) buses (load buses), must be found. The network equality constraints are represented by the load flow equations

4.2.1 Objective function

A common objective function used in OPF studies is the minimization of generation costs. The objective function based on generation operation cost can be expressed as

$$Z = \sum_{i=1}^{NG} C_i(P_i) \tag{4.6}$$

where C_i is generator's fuel cost function, which is usually quadratic and can be written as

$$C_i = a_i P_i^2 + b_i P_i + c_i$$

and NG is the set of all generating units including the generator at the slack bus.

4.2.2 Network equations

The network equations are obtained from the basic *kirchoff's laws* governing the loop flows and nodal power balance as follows

$$P_i - PD_i \pm P_{DC}^{term} = \sum_j |V_i||V_j|(G_{i,j}\cos(\delta_i - \delta_j) + B_{i,j}\sin(\delta_i - \delta_j)) \qquad \forall i = 1, ..N; j \neq slack \tag{4.7}$$

$$Q_i - QD_i - Q_{DC}^{term} = \sum_j |V_i||V_j|(G_{i,j}\sin(\delta_i - \delta_j) - B_{i,j}\cos(\delta_i - \delta_j)) \qquad \forall i = 1, ..NL \tag{4.8}$$

Where V is the bus voltage, δ is the angle associated with V, $G_{i,j}$ and $B_{i,k}$ are conductance and susceptance elements of bus admittance matrix, P and Q are real and reactive power generation respectively, PD and QD are real and reactive power demand respectively and NL is the number of P-Q buses, P_{DC}^{term} and Q_{DC}^{term} are the real and reactive power associated with the converters and the sign '+' is used when the converter at the corresponding bus is operating as inverter and '-' is used when the converter at the corresponding bus is operating as rectifier.

4.2.3 Generation limits

Generator limits are

$$P_i^{Min} \leq P_i \leq P_i^{Max} \qquad \forall i \in NG \tag{4.9}$$

$$Q_i^{Min} \leq Q_i \leq Q_i^{Max} \qquad \forall i \in NG \tag{4.10}$$

P^{Min} and P^{Max} are the upper and lower limits on real power generation and Q^{Min} and Q^{Max} upper and lower limits on reactive power generation from a unit.

4.2.4 Bus voltage limits

This constraint ensures that the voltages at different busses in the system are maintained at specified levels. The generator bus (or PV bus) voltages are maintained at a fixed level. Voltage level at a load bus is maintained within a specified upper limit V^{Max} and a lower limit V^{Min}, determined by the operator.

$$|V_i| = constant, \qquad \forall i = 1, ..., NG \tag{4.11}$$

$$V_i^{Min} \leq |V_i| \leq V_i^{max}, \forall i = 1, ..., NL \tag{4.12}$$

4.2.5 Limits on reactive power Support

This constraint may be required in case the system operator has to include decisions on optimal reactive switching at load buses.

$$QG_i^{Min} \leq QG_i \leq QG_i^{Max} \qquad \forall i \in NL \tag{4.13}$$

QG^{Min} and QG^{Max} are the limits on bus reactive power support.

4.2.6 Limits on power Flow

Transmission lines are limited by their power carrying capability, which is determined by the

$$P_{i,j} = \frac{|V_i||V_j|}{X_{i,j}} sin(\delta_i - \delta_j) \tag{4.14}$$

$$P_{i,j} \leq P_{i,j}^{Max} \tag{4.15}$$

$P_{i,j}$ is the power flow over a line *i-j* and $P_{i,j}^{Max}$ is the maximum limit on power flow over the line.

4.2.7 DC terminal voltage equations

Using the per unit system, the average value of the DC voltage of a converter connected to bus *fr* is

$$V_{dr} = \frac{3\sqrt{2}}{\pi} t_1 V_{fr} \cos\alpha \tag{4.16}$$

and incase if the converter is operating as inverter then the DC voltage can be written as

$$V_{di} = \frac{3\sqrt{2}}{\pi} t_2 V_{to} \cos\gamma \tag{4.17}$$

4.2.8 Firing angle limits

These constraints ensure that the limits on the ignition delay angle and the extinction advance angle of the rectifier and the inverter are maintained within specified limits.

$$\cos\alpha \leq \cos\alpha^{max} \qquad ; \qquad \cos\alpha \geq \cos\alpha^{min}$$

As mentioned earlier adequate α is required so as to provide sufficient voltage across thyristor at the time of firing. similarly at inverter side

$$\cos\gamma \leq \cos\gamma^{max} \qquad ; \qquad \cos\gamma \geq \cos\gamma^{min}$$

4.2.9 Transformer tap changer limits

There will be a minimum and maximum limit on the transformer tap changer settings above which may leads to infeasible solution or not possible because of some constraints.

$$t1 \leq t_1^{max} \qquad ; \qquad t_1 \geq t1^{min}$$

$$t2 \leq t_2^{max} \qquad ; \qquad t_2 \geq t2^{min}$$

4.3 Characteristic Features of OPF

The main features of an OPF is its ability to include the detailed network configuration and bus-wise demand balance for both active and reactive power. The OPF can include many operating constraints and model other issues also. Specifically limits on reactive power generation in addition to real power generation, power flow limits on the transmission lines and limits on the bus voltages ensure that the system is operated in a secure manner.

4.4 OPF Applications

One of the main feature of the OPF is that it is a flexible analytical tool, which allows the use of different objective functions to solve different problems. The objective functions commonly used for operation and planning studies are as follows

- Minimize cost of operation
- Minimize the deviation or minimize control shift
- Loss minimization
- Minimize the cost of installation of new capacitors and reactors and/or cost of MVAr supplied
- Maximum transfer capacity
- Minimize the emissions, and so on.

4.5 Results and Discusions

A 14 bus system is considered for AC-DC OPF simulations. The simulation study involves the use of MATLAB and GAMS for optimizing the power flow. GAMS is mainly used for optimization of an objective function with respect to a set of constraints. It models and solves complex linear, nonlinear and quadratic problems. Here point-to-point and multiterminal configurations have been considered. Table 4.1 to Table 4.3 indicates the general data for all HVDC configurations.

Line data and bus data of the system considered are shown in Table 4.1 and Table 4.2 respectively. The generator's fuel cost function coefficients is shown in Table 4.3. The lower limit on generator output is considered as 15 MW. Lower limit on firing angles of converters is taken as 15^o. The lower and upper limits of transformer tap positions located at converters are taken as 0.7 p.u and 1.3 p.u for point-to-point, multiterminal radial and 0.6 p.u and 2.0 p.u for multiterminal series connection. The input to the GAMS is passed from a MATLAB program through the MATGAMS interface. After optimizing the given objective function w.r.t constraints in GAMS, the result can be obtained MATLAB.

Programs have been written in GAMS software for the optimization of generation cost of power producing for the case of point-to-point DC transmission line and multiterminal HVDC line. Here equality and inequality constraints have been considered as discussed in Section 4.2. The written GAMS programs have been interfaced with MATLAB

Table 4.1: Line Data

From Bus	To Bus	R (p.u)	X (p.u)	B/2 (p.u)	Flow Limit (p.u)
1	2	0.01938	0.05917	0.0264	3
1	5	0.05403	0.22304	0.0246	3
2	3	0.04699	0.19797	0.0219	3
2	4	0.05811	0.17632	0.0170	3
2	5	0.05695	0.17388	0.0173	3
3	4	0.06701	0.17103	0.0064	3
4	5	0.01335	0.04211	0.0	3
4	7	0.0	0.20912	0.0	3
4	9	0.0	0.55618	0.0	3
5	6	0.0	0.25202	0.0	3
6	11	0.09498	0.19890	0.0	3
6	12	0.12291	0.25581	0.0	3
6	13	0.06615	0.13027	0.0	3
7	8	0.0	0.17615	0.0	3
7	9	0.0	0.11001	0.0	3
9	10	0.03181	0.08450	0.0	3
9	14	0.12711	0.27038	0.0	3
10	11	0.08205	0.19207	0.0	3
12	13	0.22092	0.19988	0.0	3
13	14	0.17093	0.34802	0.0	3

In Table. 4.2, bus type 1,2 and 3 indicates slack bus, PV (generator) and PQ (load bus) respectively.

4.5.1 Point-to-point DC transmission line

An HVDC line is included between buses 7 and 10. The converters at bus 7 and at bus 10 operate in rectifier and inverter mode respectively. Simulations result for point-to-point DC line are shown in Table 4.4 to Table 4.6.

Table 4.4 indicates optimized generator outputs, bus voltage magnitudes and angles.

Table 4.2: Bus Data

Bus	Type	Vsp (p.u)	δ (radians)	P_{Gi} (MW)	Q_{Gi} (MVAR)	P_{Li} (MW)	Q_{Li} (MVAR)	Q_{min} (MVAR)	Q_{max} (MVAR)
1	1	1.020	0	0	0	14	0	-10	20
2	2	1.025	0	100	42.4	21.7	12.7	-50	40
3	2	1.010	0	100	23.4	94.2	19.0	-60	100
4	2	1.045	0	90	12.2	11.2	7.5	0	100
5	2	1.010	0	60	17.4	0.0	0.0	-60	10
6	3	1.0	0	0	0	47.8	-3.9	0	0
7	3	1.0	0	0	0	7.6	1.6	-50	300
8	3	1.0	0	0	0	0.0	0.0	0	0
9	3	1.0	0	0	0	29.5	16.6	0	0
10	3	1.0	0	0	0	9.0	5.8	-300	300
11	3	1.0	0	0	0	3.5	1.8	0	0
12	3	1.0	0	0	0	6.1	1.6	0	0
13	3	1.0	0	0	0	13.5	5.8	0	0
14	3	1.0	0	0	0	14.9	5.0	0	0

Table 4.3: Coefficients for Cost Functions of Generators

Bus No.	a (\$/MW^2)	b (\$/MW)	c (\$)
1	0.0095	10	150
2	0.0095	15	220
3	0.0095	17	230
4	0.0095	14	200
5	0.01	18	200

This table shows that all bus voltage values are within permissable limits of ± 5% according to the standards and generators real power are within limits.

The optimized values of firing angles, transformer tap positions, current through the DC line are shown in Table 4.5 for the specified values of voltage (V_i) and real power (P_{di}) at inverter side.

Table 4.6 is presented to show the status of the optimization. In this table model status 2 indicates the objective is locally optimal and solver status indicates the code has been compiled normally. It also indicates the optimized cost for all generator is 1030.01 \$/MW.

Hence, from the above discussion it is clear that the written code for the optimization

Table 4.4: Point-to-point DC Transmission Result

Generator output (p.u)	Bus voltage magnitude (p.u)	Bus voltage angles (radians)
2.0368	1.0200	0.0843
0.1500	1.0250	0.0000
0.1500	1.0100	-0.1108
0.1500	1.0450	-0.0854
0.1500	1.0100	-0.0520
0	1.0354	-0.1887
0	0.9500	-0.2140
0	0.9500	-0.2140
0	1.0326	-0.1768
0	1.0500	-0.1309
0	1.0423	-0.1624
0	1.0270	-0.2053
0	1.0252	-0.2065
0	1.0191	-0.2116

Table 4.5: DC Variables in Point-to-point Connection

Alpha (Degrees)	Gamma (Degrees)	t_1 (p.u)	t_2 (p.u)	I_d (p.u)	V_r (p.u)	V_i (p.u)	P_{di} (p.u)
14.9943	14.9943	0.9858	0.8764	0.7083	1.2212	1.2000	0.8500

Table 4.6: GAMS Status and Objective Value

Modelstatus	Solvestatus	Objective
2	1	1030.01

has been achieved successfully.

4.5.2 Multiterminal HVDC

The optimization code has been written for the two configurations of multiterminal HVDC as discussed in Chapter 2.

1) Multiterminal series connection

Four converters are considered in multiterminal series connection which is discussed in Section 3.5. Rectifier (Rec) and inverter (Inv) are connected at buses 7 and 10 respectively.

Table 4.7: Multiterminal Series Connection Result

Generator output (p.u)	Bus voltage magnitude (p.u)	Bus voltage angles (radians)
2.3000	1.0200	0.0930
0.2725	1.0250	0.0000
0.1500	1.0100	-0.1208
0.9000	1.0450	-0.1043
0.1500	1.0100	-0.0703
0	1.0473	-0.2522
0	1.0500	-0.3614
0	0.9500	-0.3614
0	1.0316	-0.2939
0	1.0500	-0.2419
0	1.0474	-0.2501
0	1.0388	-0.2723
0	1.0350	-0.2773
0	1.0226	-0.3084

Table 4.8: DC variables in Multiterminal Series Connection

Alpha (Degrees)	Gamma (Degrees)	t_{rec} (p.u)	t_{inv} (p.u)	t_{inv1} (p.u)	t_{inv2} (p.u)	I_d (p.u)	V_r (p.u)	V_i (p.u)	P_{di} (p.u)
14.9943	14.9943	1.9294	0.8034	0.6000	0.6000	0.7273	2.6418	1.1000	0.8000

Table 4.9: GAMS Status and Objective Value

Modelstatus	Solvestatus	Objective
2	1	1045.00

Tables 4.7, Table 4.8 and Table 4.9 show the simulation results for the OPF for multiterminal series connection. Tables 4.7 indicates that all bus voltages and generators outputs are in well-preserved limits. The optimized values of firing angles, transformer tap positions and current through the DC line are shown for the specified voltage and power at inverter are shown in Table 4.8. Table 4.9 indicates the written program in GAMS executed successfully and the optimized cost is found to be 1045.00 $/MW.

2) Multiterminal radial connection

Four converters are considered in multiterminal radial connection which is discussed in Section 3.5. Rectifiers, Rec1 and Rec2 are connected at buses 7 and 10 respectively.

Table 4.10: Multiterminal Radial Connection Result

Generator output (p.u)	Bus voltage magnitude (p.u)	Bus voltage angles (radians)
2.3000	1.0200	0.0872
0.7275	1.0250	0.0000
0.1500	1.0100	-0.1345
0.9000	1.0450	-0.1304
0.1500	1.0100	-0.0972
0	1.0500	-0.3393
0	1.0500	-0.3941
0	0.9500	-0.3941
0	1.0324	-0.3978
0	1.0245	-0.4145
0	1.0350	-0.3809
0	1.0417	-0.3607
0	1.0374	-0.3668
0	1.0241	-0.4059

Table 4.11: Firing Angles of Converters in Multiterminal Radial Connection

Alpha1 (Degrees)	Alpha2 (Degrees)	Gamma1 (Degrees)	Gamma2 (Degrees)
14.9943	14.9943	14.9943	14.9943

Table 4.12: Transformer Tap positions at Converters in Multiterminal Radial Connection

t_{rec1} (p.u)	t_{rec2} (p.u)	t_{inv1} (p.u)	t_{inv2} (p.u)
0.8332	0.8540	0.9373	0.9373

Tables from 4.10 to 4.14 indicate the simulation results for the OPF for multiterminal radial connection. From these tables, it is observed that the voltages and output of

Table 4.13: Voltages, Currents and Real Powers in Multiterminal Radial Connection

I_{r1} (p.u)	I_{r2} (p.u)	I_{i1} (p.u)	I_{i2} (p.u)	V_r (p.u)	V_i (p.u)	P_{di1} (p.u)	P_{di2} (p.u)
1.1007	0.2629	0.7273	0.6364	1.1409	1.1000	0.8000	0.7000

Table 4.14: GAMS Status and Objective Value

Modelstatus	Solvestatus	Objective
2	1	1051.83

generators are within boundary limits. Hence, optimization is achieved successfully with optimization cost of 1051.83 \$/MW.

Chapter 5

Conclusions and Future Scope of Research

5.1 Conclusions

There has been a growing interest in HVDC technology since the first HVDC installation took place in Gotland, sweeden, in 1954. The high flexibility of control available with HVDC transmission results in a number of new advantages and applications which have been presented in Chapter 2. The main objective of the thesis is to perform load flow and optimal power flow analysis of an AC-DC system. Here, load flow analysis for different configurations of single and multiple DC transmission line are discussed.

MATLAB simulations are carried out for point-to-point DC transmission for various operating modes. These modes are defined by considering any three out of the seven DC variables specified for a particular power transfer through the DC line. The respective modes of operation are discussed in detail in Section 3.4. Transition from one mode to another mode takes place if any unspecified variable exceeds its boundary limits. Then, HVDC operating mode shifts to a new mode. Under the transition between modes, the variable which exceeds its operating limit is fixed at that limit and any one of the fixed variables in the transiting mode is made free to be varied.

The following results are observed from the case studies carried out.

(1) The reactive power consumed by converters is minimum when HVDC is operating in modes where α_{min}, γ_{min}, $V_{di}/V_{dr}/t_1/t_2$ are specified. Also, current flowing through the DC line depends on the specified value of tap position of the converter transformer.

(2) HVDC operation is practically not feasible for some modes. This is explained in detail in Section 3.5.

(3) Simulations also involve the transition of operating modes under the case of priorities of them given as one of the inputs. The transition between operating modes took place successfully.

Simulations for series and radial configurations of multiterminal HVDC line are also carried out. In case of the series configuration, the range of transformer tap positions required is significantly greater than that in case of radial configuration. This directly effects the cost of transformer and it is explained in detail in Section 3.5. In case of any converter failure, partial power can be transferred using a radial configuration, whereas it leads to complete interruption of power in case series configuration. Therefore, radial configuration is much superior and is preferred in practical systems.

Apart from simple load flow studies, an optimal power flow study is also carried out for the AC-DC system. The OPF model is developed by using a generalized matrix representation of the HVDC link. The OPF calculation is performed by using GAMS. The input to the GAMS program is passed from a MATLAB program through the MATGAMS interface. Simulation results validated the satisfactory operation of an AC-DC system such as, maintaining voltages at all buses within 5 % tolerance level, transferring line power within acceptable limits. Moreover, it also ensures the correct direction of converter currents.

5.2 Future Scope of Research

In the present work, steady state analysis of AC-DC system is done. Based on the work done, it can be concluded that a number of applications and advancements in HVDC transmission system are required, which are mentioned below.

1. Analysis of transient behavior of interconnected AC-DC system under switching and fault conditions can be done.

2. A generic concept of modeling of all types of HVDC systems considering all the possible configurations is needed. This can reduces the complexity involved in analyzing the power system.

3. Effective utilization of VSC in an interconnected AC-DC system can be sought for the integration of DC sources with the utility grid.

Bibliography

[1] K. Meah and Sadrul Ula, "Comparative Evaluation of HVDC and HVAC Transmission Systems," in *Power Engineering Society General Meeting*, pp. 1-5, 2007.

[2] Prabha Kundur, *Power System Stability and Control*. New York: Tata Mcgraw-Hill Edition, pp. 463-579. 1994.

[3] J. Arrillaga, Y. H. Liu, and N. R. Watson, *Flexible Power Transmission: The HVDC Options*. England: John wiley and sons Ltd, pp. 21-95.

[4] J. Setreus and L. Bertling, "Introduction to HVDC Technology for Reliable Electrical Power Systems," in *Probabilistic Methods Applied to Power Systems*, pp. 1-8, 2008.

[5] Y. Tzeng, Nanming Chen, and Ruay-Nan Wu, "A Detailed R-L Fed Bridge Converter Model for Power Flow Studies in Industrial AC/DC Power Systems," *IEEE Transactions on Industrial Electronics*, vol. 42, no. 5, pp. 531-538, October 1995.

[6] E. W. Kimbark, *Direct Current Transmission*. New York: wiley interscience, vol. 1, pp. 21-95, 1971.

[7] P. G. Engstrom, "Operation and Control of HVDC Transmission," *IEEE Transactions on Power Apparatus and Systems*, vol. 83, no. 1, pp. 71-77, 1964.

[8] Lidong Zhang and L. Dofnas, "A novel method to mitigate commutation failures in HVDC systems," in *Power System Technology*, vol. 1, pp. 51-56, 2002.

[9] D. A. Braunagel, L.A. kraft, and J.L. Whysong, "Inclusion of DC converter and transmission equations directly in a Newton power flow," *IEEE Transactions on Power Apparatus and Systems*, vol. 95, no. 1, pp. 76-88, 1976.

[10] H.A. Sanghavi and S. K. Banerjee, "Load Flow Analysis of AC - DC Power Systems," in *TENCON' 89*, pp. 746-751, 1989.

[11] J. Arrillaga and B. Smith, *AC-DC power system analysis*. London, United Kingdom: IET, pp. 61-107, 1998.

[12] F. Coffele, R. J. Garcia-Valle, and E. Acha, "The Inclusion of HVDC Control Modes in a Three-Phase Newton-Raphson Power Flow Algorithm," in *Power Tech*, pp. 419-424, 2007.

[13] T. Smed, G. Andersson, G.B. Sheble, and L. L. Grigsby, "A new approach to AC/DC power flow," *IEEE Transactions on Power Systems*, vol. 6, no. 3, pp. 1238-1244, 1991.

[14] A. Ekstrom, "A Refined HVDC Control System," *IEEE Transactions on Power Apparatus and Systems*, vol. 89, no. 5, pp. 723-732, 1970.

[15] J. Reeve, "Multiterminal HVDC Power Systems," *IEEE Transactions on Power Apparatus and Systems*, vol. 89, no. 2, pp. 729-737, 1980.

[16] R. Foerst, G. Heyner, K. W. Kanngiesser, and H. Waldamnn "Multiterminal Operation of HVDC Converter Stations," *IEEE Transactions on Power Apparatus and Systems*, vol. 88, no. 7, pp. 1042-1052, 1969.

[17] V. F. Lescale, A. Kumar, L. E. Juhlin, H. Bjorklund, and K. Nyberg, "Challenges with Multi-Terminal UHVDC Transmissions," in *Power System Technology and IEEE Power India Conference*, pp. 1-7, 2008.

[18] J. P. Bowles, H. L. Nakra, and A. B. Turner, "A Small Series Tap on an HVDC Line," *IEEE Transactions on Power Apparatus and Systems*, vol. 100, no. 2, pp. 857-862, 1981.

[19] K. Bhattacharya, M. H. J. Bollen, and J. Daalder, *Operation of Restructured Power Systems*. New York: Kluwer Academic Publication, pp. 30-40, 2001.

[20] B. Warkad, M. K. Khedkar, and G. M. Dhole "A genetic algorithm approach for solving AC-DC optimal power flow problem," *Journal of Theoretical and Applied Information Technology*, vol. 16, no. 1, pp. 027-039, 1981.

[21] C. N. Lu, S. S. Chen, and M. Ong, "The Incorporation of HVDC equations in optimal power flow methods using sequential quadratic programming techniques," *IEEE Transactions on Power Systems*, vol. 3, no. 3, pp. 1005-1011, August 1988.